agronomy

MDPI

Article

Geochemical Profiles of Deep Sediment Layers from the Kolubara District (Western Serbia): Contamination Status and Associated Risks of Heavy Metals

Milica Vidak Vasić [1,*], Milena Radomirović [2], Pedro M. Velasco [3,4] and Nevenka Mijatović [1]

[1] Centre for Materials, Institute for Testing of Materials IMS, Bulevar Vojvode Mišića 43, 11000 Belgrade, Serbia; nevenka.mijatovic@institutims.rs
[2] Innovation Center, The Faculty of Technology and Metallurgy, University of Belgrade, Karnegijeva 4, 11120 Belgrade, Serbia; mradomirovic@tmf.bg.ac.rs
[3] Escuela Superior de Ingeniería y Tecnología, Universidad Internacional de La Rioja, Avda. de la Paz, 137, 26007 Logroño, Spain; pedro.munoz@unir.net
[4] Facultad de Ingeniería, Universidad Autónoma de Chile, 5 Poniente, Talca 1760, Chile
* Correspondence: milica.vasic@institutims.rs

Abstract: Global awareness of the harmful effects of heavy metal contamination in soil has increased significantly. Understanding the vertical distribution of oxides and elements is vital for tracing the history of potential contamination. Thus, this study focuses on deep sediment cores primarily composed of quartz and clay minerals from a small village in the western Tamnava Basin of Serbia. The aim was to assess the vertical distribution of 11 oxides and 21 elements and the ecological risks of eight heavy metals by analyzing 250 sediment samples from 18 boreholes at depths ranging from 5 to 58.5 m. Deep sediment core samples were analyzed using energy-dispersive X-ray fluorescence spectrometry (ED-XRF). Potential contamination levels were evaluated within the study area. Additionally, samples were analyzed for total carbonate and organic carbon contents and particles retained on a 0.063 mm sieve. Higher than permitted concentrations of vanadium (V), thallium (Tl), and barium (Ba) were found. Notably, this zone is located above a proposed lithium and boron mine in Gornje Nedeljice, making it crucial for monitoring efforts. Even if mining operations do not commence, examining the deep sediment layers in this rural area remains important. This study offers novel and valuable data on the concentrations of potentially toxic elements in undisturbed deep sediment, serving as a benchmark for future comparisons.

Keywords: geochemical composition; rural sediment layers profiles; vertical contamination distribution; multi-index approach; ecological risk assessment; western Serbia

check for updates

Citation: Vasić, M.V.; Radomirović, M.; Velasco, P.M.; Mijatović, N. Geochemical Profiles of Deep Sediment Layers from the Kolubara District (Western Serbia): Contamination Status and Associated Risks of Heavy Metals. *Agronomy* **2024**, *14*, 3009. https://doi.org/10.3390/agronomy14123009

Academic Editor: Bing Li

Received: 22 November 2024
Revised: 11 December 2024
Accepted: 16 December 2024
Published: 18 December 2024

Copyright: © 2024 by the authors. Licensee MDPI, Basel, Switzerland. This article is an open access article distributed under the terms and conditions of the Creative Commons Attribution (CC BY) license (https://creativecommons.org/licenses/by/4.0/).

1. Introduction

A pollution control system must incorporate comprehensive monitoring, which includes systematic data collection on heavy metal concentrations within specific environments. Geochemical data play a crucial role in understanding the environmental and anthropogenic influences on soil composition and contamination [1,2]. In the western regions of the Republic of Serbia, various factors put pressure on the soil, such as urban expansion, pollution from industry and agriculture, erosion, and extreme weather events related to climate change [3]. Traditional methods for assessing the distribution of metals in soil usually involve sampling at various depths. However, soil heterogeneity can cause significant variability in the vertical distribution of metals, making it difficult to identify the key influencing factors. Besides soil characteristics, various human-made factors, such as the release and distribution of pollutants, also impact metal concentrations [4,5]. The examination of heavy metals (HMs) in soil has gained importance due to their harmful effects on ecosystems and potential risks to human health. Due to their toxicity, persistence,

and bioaccumulation potential, as well as their capacity to move through food chains, heavy metals are recognized as highly hazardous soil pollutants. The United States Environmental Protection Agency (USEPA) classifies them as priority inorganic contaminants. Excessive accumulation of these pollutants in soil can impair its productivity and pose potential risks to human health [6,7]. Furthermore, the increasing levels of heavy metal contamination present significant challenges to the region's sustainable development, as they disrupt ecological stability and jeopardize the safety of residents [5,8–10]. The presence of HMs with potential toxic effects, such as As, Cd, Cr, Cu, Hg, Ni, Pb, and Zn can lead to long-term environmental damage, particularly in regions experiencing both natural and human-induced changes [11]. Previous studies on the distribution of elements in soils have primarily concentrated on their horizontal distribution in surface layers (topsoil and subsoil), with limited focus on the comprehensive vertical distribution of elements, and oxides (including potentially toxic elements) in deep sediment cores. Namely, earlier studies have examined elemental contents and their vertical distribution, focusing on soil layers at shallower depths (up to 6 m) [12–14]. To the current knowledge, there is a noticeable gap in research on assessing environmental pollution from potentially toxic elements and their distribution in deep sediment cores, worldwide and in Serbia.

This study was prompted by the recent activities surrounding the proposed opening of a 750 m underground lithium and boron mine in Gornje Nedeljice village. The plan to establish a 220-hectare mine under high-quality agricultural land has sparked significant concern among scientists and professionals due to potential environmental risks and the substantial reserves of clean underground water in the region. The mine was projected to generate around 57 million tons of tailings over its planned 40-year operation. The initial studies showed that the exploration test activities caused increased levels of arsenic, lithium, and boron in the Jadar River and its surrounding soil [15]. Based on the average for 2017–2018, groundwater accounted for 73.3% of the Republic of Serbia's water resources, while it was utilized for 62% of the total drinking water supply [16]. Groundwater sources are considered a water resource of regional importance. However, at the same time, it can be a significant cause of morbidity and mortality due to its consumption in areas close to mining activities [15].

The Republic of Serbia with its diverse geological landscape, offers significant opportunities for geological studies, especially in rural regions that have remained relatively unindustrialized [11,17]. The Kolubara district, located in western Serbia, is of particular interest due to its importance as a mining and agricultural region. The Tamnava Basin, located in the Kolubara district, is mainly a rural area with limited industrial activity. Its geological characteristics and the presence of clays and other fine sediments make it an ideal site for studying baseline contamination levels and the potential accumulation of heavy metals [18]. Previous studies in Serbia and other Balkan countries have focused on soil contamination near industrial zones, mining sites, and urban areas, leaving rural regions underexplored [19–23]. In particular, while research on the Kolubara coal basin has provided insights into air and water pollution from mining activities, there has been little focus on the long-term accumulation of heavy metals in rural deep sediment profiles [24]. However, limited studies have been conducted to assess the broader environmental impact of heavy metal contamination in the Kolubara region's soil. Despite some attempts to study the deposition of heavy metals from industrial sources, there is still a lack of understanding regarding the vertical distribution of these contaminants in rural and semi-rural areas, particularly in regions not directly impacted by heavy industry [25]. Another significant aspect of this work is that, to the best of our knowledge, no other study analyzed sediments to such depths. This study addresses this gap by analyzing 250 sediment samples from 18 boreholes, focusing on the vertical distribution of oxides and heavy metals across a depth of up to 58.50 m.

In this study, the vertical sediment profiles of different land types by use (meadow and agricultural land of class VI, and pasture of class III) were collected and analyzed for the concentrations of 11 oxides and 21 elements. Various indexes were employed

to assess sediment contamination levels. Moreover, to understand how deep sediment composition affects the retention of heavy metals, the total carbonate content and residual fraction remaining on a 0.063 mm sieve were determined. The main objectives of this study were to (1) explore the levels and vertical distributions of elements and oxides in deep undisturbed sediment layers for the first time; (2) evaluate the deep sediment enrichment and contamination status posed by HMs; and (3) analyze the potential sources of the analyzed elements and oxides. By studying rural areas distant from major industrial sources and the deep sediment layers of up to 58.5 m, this research seeks to establish an environmental benchmark that can be used for long-term ecological monitoring and sustainable land management in the Kolubara and Tamnava regions.

2. Materials and Methods

2.1. Study Area and Sample Collection

The 250 samples were collected from 18 boreholes in Gornje Crniljevo, from the northeastern slopes of Vlašić Mountain within the Osečina municipality in Western Serbia (Figure 1, Table A1). The village is located on the left bank of the Tamnava River, close to the Osečina–Kamenica road. Gornje Crniljevo is part of the Tamnava region, situated within the Savinian-Tamnava Tertiary Basin. This basin is characterized by sedimentary mineral layers that accumulated during the Neogene period (23 to 2.6 million years ago) and is rich in clay minerals and other sedimentary deposits. Stratigraphically, this formation is classified as Upper Miocene, specifically within the Pannonian layer and its associated freshwater deposits. From a lithological perspective, the upper Miocene sediments of Gornje Crniljevo primarily consist of clay, sandy clay, rarely carbonaceous clay, then sand, clayey sand and less often gravel [26,27]. According to the mineralogical composition, the clay minerals belong to the illite–kaolin type. The layers are mostly horizontal, although locally they can have a slight dip that depends on the paleo-relief. The region under study is classified as having a moderate to high level of underground water threat, as indicated by the Ministry of Mining and Energy of the Republic of Serbia [26,27]. It is important to highlight that this region has rich groundwater resources and is also prone to erosion. In the Republic of Serbia, a total of 2228 landslides and unstable slopes have been documented on the territory of 28 municipalities, including the municipalities of Osečina, Valjevo, and Loznica in western Serbia [28].

The relief of the terrain is hilly, covered with forest vegetation, meadows, and pastures. The terrain morphology of the wider area is mountainous, with an elevation difference of 221 m. The highest point is at the "Kriva Glava" location (399 m), while the lowest lies in the Tamnava River valley (178 m) in the area of Donje Crniljevo. The area is abundant in springs and watercourses. The most significant watercourse is the Tamnava River, which flows into the Kolubara River and is part of the Black Sea basin. The closest water course is the Tamnavica River, which belongs to the Sava River Basin. The Tamnava River is formed by the Tomin Stream and the Tamnavica, with its main tributary being the Miličinica River. The climate in this region is moderately continental, characterized by warm summers and cold winters.

The samples were collected using the usual technique of drilling cylindrical holes with appropriate equipment using a PVC tube to avoid contamination. The topsoil and subsoil layers of 5 m are removed since the organic matter is mainly present in this part of the material. The core-shaped samples were wrapped with self-adhesive foil immediately after collection and sealed. The boreholes studied in this work were assigned BC-10 to BC-27, covering a depth from 5.0 to 58.5 m (Figure 1). The surface described by the selected exploratory boreholes is 573,439 m^2, of which 490,419 m^2 is declared as agricultural land of the classes V to VII and pastures of the class III. The purpose of the land studied in the selected boreholes is noted in Table 1.



Figure 1. The position of Gornje Crniljevo (Vlašić Mountain) and geological map with sampling sites.

Table 1. Tested boreholes and the purpose of land.

Borehole	Purpose	Borehole	Purpose
BC-10	Meadow, class VI	BC-19	Agricultural field, class VI Meadow, class VI
BC-11	Meadow, class VI	BC-20	Meadow, class VI
BC-12	Agricultural field, class VI	BC-21	Meadow, class VI
BC-13	Agricultural field, class VI	BC-22	Meadow, class VI
BC-14	Agricultural field, class VI	BC-23	Agricultural field, class VI
BC-15	Meadow, class VI	BC-24	Agricultural field, class VI
BC-16	Meadow, class VI	BC-25	Meadow, class VI
BC-17	Agricultural field, class VI	BC-26	Pasture, class III
BC-18	Agricultural field, class VI	BC-27	Agricultural field, class VI

2.2. Sample Preparation and Analysis

The deep sediment samples underwent a series of preparation steps. These steps included drying, grinding, and homogenization. A detailed description of the analytical procedure can be found in the work of Mijatović et al. [29]. The samples were sieved through a 0.063 mm mesh to determine the sand-sized fraction quantity, with the remaining material representing the clay and silt (alevrolite)-sized components of the sample [30].

Using the non-purgeable method, the element analyzer TOC-VCPN was used to determine the total organic carbon content (TOC). In the initial analysis stage, the sample was acidified using a syringe with 2 M of HCl. Next, the carrier gas was passed through the sample to remove any carbonates that might be present. The sample was then injected into the instrument's oven and heated to 680 °C. The detector was a non-dispersive infrared gas analyzer.

The energy-dispersive X-ray fluorescence (ED-XRF) method is a non-destructive technique widely used to determine the elemental composition of soils, enabling precise multi-element analysis. This technique is increasingly applied in environmental studies due to its efficiency in detecting trace levels of heavy metals and oxides in soil samples [29–31]. In this study, the chemical composition was analyzed using the ED-XRF technique with the Spectro Xepos instrument, equipped with a 50 W/60 kV X-ray tube (Ametek, Meerbusch, Germany). The analysis was performed using the fired pellets method based on fundamental parameters [29]. To ensure the reliability of the method, calibration and validation were conducted using a series of certified reference materials (CRMs), including CRM-07402 and CRM-2709 (Institute of Geophysical and Geochemical Exploration, Langfang, China), CRM-2710 (National Institute of Standards and Technology, Gaithersburg, MD, USA), NCS DC 60102 (China National Analysis Center for Iron and Steel, Beijing, China), CRM-07427, CRM-07428, CRM-07430, NCS DC 60104, NCS DC 60105, and NCS DC 60106 (National Research Centre for Certified Reference Materials, Beijing, China). This approach facilitated accurate elemental analysis of the tested samples and ensured robust results. The validation of the ED-XRF method encompassed the determination of the Limits of Detection (LOD) and the Limits of Quantification (LOQ) based on calibration curves. The LOD values ranged from 0.001% (Mn) to 1.56% (Si), whereas the LOQ values ranged from 0.004% (Mn) to 4.73% (Si). These values confirm the method's sensitivity for detecting both major and trace elements. Trueness was assessed by comparing the measured concentrations of CRM samples with their certified values. The results demonstrated recovery rates within the acceptable range of 89% to 115%, ensuring reliable quantification. Precision was evaluated through repeatability and reproducibility tests. The relative standard deviation (RSD) for repeatability ranged from 0.23% (Ca and Mn) to 3.82% (Mg), while reproducibility ranged from 0.42% (K) to 4.56% (S). Analyses were performed in triplicate, on different days, by multiple analysts, with ANOVA used to evaluate reproducibility. Total measurement uncertainty was calculated by combining the uncertainties associated with sample preparation, calibration, and instrument precision. The expanded uncertainty was expressed at a 95% confidence level, using a coverage factor of 2. Total uncertainties ranged from 3.64%

(Fe) to 8.21% (Na), with the highest uncertainties observed for light elements due to their shallower analytical depths.

In deep sediment samples, the weight loss at 1000 °C is owed to the combustion of organic components, the disintegration of carbonates, and the decomposition of clay minerals during the firing process, thereby forming new mineral phases. It is a necessary parameter to obtain in the complete XRF analysis because the resulting chemical composition is recalculated accordingly. This value is presented by the loss on ignition (LOI) and was determined by weighing the specimens before and after they were heated in a muffle furnace. Furthermore, milled and dried samples were tested to discover the residue on the 0.063 mm sieve by the wet method. The total amount of magnesium and calcium carbonates (CCC) was determined using Scheibler's volumetric method. Both CCC and TOC are related to LOI, as seen in Pearson's correlation analysis. Although not usually used in the studies of soil contamination monitoring, these parameters (LOI and CCC) complement each other and serve for verification in the study of deep sediments in this work.

Recent research highlights the crucial role of clay minerals and carbonates in restricting contaminant migration, serving as natural barriers in soils [32,33]. The significance of carbonate analysis has been emphasized in the recent studies of sedimentary soils [34,35]. In samples from the Kolubara district, carbonates can notably affect soil pH and buffering capacity, influencing the mobility of heavy metals [36]. Similar approaches have been applied in European studies, such as Răcușan Ghircoiaș et al. [37], which examined rural soils not directly impacted by industrial activities but still exhibiting elevated contaminant levels due to atmospheric deposition.

In the summary, the database includes the depths from/to, layer thickness, RS, CCC, TOC, oxide and microelement contents.

2.3. Contamination Status and Ecological Risk Assessment of Deep Sediment Samples

Most commonly used indexes in practice to assess soil and/or sediment contamination levels by heavy metals (As, Cd, Cr, Cu, Hg, Pb, Ni, Zn) include single indices, like the enrichment factor (EF) and contamination factor (CF), as well as integrated indices, such as the pollution load index (PLI) and potential ecological risk index (RI) [7,12,30]. To determine the degree of contamination for each potentially toxic element at a particular site, the contamination factor [30] and enrichment factor are employed as individual indices. The essential difference between these two indices is that the CF is based on the baseline value of the element, while the EF additionally takes into account the element baseline concentration, as well as the baseline (background) of the reference element [38]. The background metal concentrations from the continental crust reported by Taylor (1964) were used [39].

Enrichment factors (EF) are typically determined by comparing heavy metal concentrations to their geochemical background values [39], including the baseline concentration of a chosen reference element. Reference elements such as Al, Mn, and Fe are commonly used to account for mineralogical effects; in this study, Mn was selected as the reference element [40]. This index provides a key measure for assessing the impact of anthropogenic activities on heavy metal levels [12] and can indicate whether individual metal enrichment is present due to natural processes or human activities. Table 2 provides the classification of enrichment levels along with detailed explanations for the letters used in the formula.

The contamination factor (CF) reflects the ratio between the concentrations of heavy metals and their geochemical background. Contamination levels are categorized into four groups (Table 2), which quantify the level of contamination of each metal at a given site.

Table 2. Pollution indexes, classification, and pollution risk levels.

Indexes	Equations	Description	Pollution Risk Level	References
Pollution indexes				
Contamination factor (CF)	$C_f^i = \frac{C^i}{C_n^i}$	C_n^i is the pre-industrial value of an element (i); C_i is the content of the element (i)	CF < 1 → Low contamination 1 < CF < 3 → Moderate 3 < CF < 6 → Considerable CF ≥ 6 → Very high	[38,41]
Enrichment factor (EF)	$EF = \left[\frac{Ci}{Cref}\right] sample / \left[\frac{Ci}{Cref}\right] background$	C_i is the content of an element (i); C_{ref} is the content of the reference element (Mn) for geochemical normalization.	EF < 2 → Minimal enrichment 2 ≤ EF < 5 → Moderate 5 ≤ EF < 20 → Significant 20 ≤ EF < 40 → Very high EF ≥ 40 → Extremely high enrichment	[40,42,43]
Pollution load index (PLI)	$PLI = \sqrt[n]{CF_1 \times CF_2 \times CF_3 \times \ldots \times CF_n}$	CF_n is the contamination factor value obtained based on the ratio of the measured element concentration and its corresponding reference value [39]; n is the number of analyzed elements (n = 9)	PLI = 0 → No contamination 0 < PLI < 1 → Baseline contamination PLI > 1 → High contamination	[41,44,45]
Ecological risk indexes				
Ecological risk factor (Er)	$E_r^i = T_r^i \times C_f^i$	T_r^i is the toxicity response coefficient of element (i) (As = 10; Cd = 30; Cr = 2; Cu = 5; Hg = 40; Ni = Pb = 5; Zn = 1); C_f^i denotes the contamination factor of the individual element (i)	E_r < 40 → Low potential ecological risk 40 ≤ E_r < 80 → Moderate 80 ≤ E_r < 160 → Considerable 160 ≤ E_r < 320 → High E_r ≥ 320 → Very high potential ecological risk	[38]
Potential ecological risk index (RI)	$RI = \sum_{i=1}^{n} E_r^i$	$\left(E_r^i\right)$ is the potential ecological risk factor of a single element (i) (n) is the number of studied elements (n = 8 in this study); *RI* is the index of potential ecological risk parameters of all toxic elements	RI < 150 → Low ecological risk 150 ≤ RI < 300 → Moderate 300 ≤ RI < 600 → Considerable RI ≥ 600 → Very high ecological risk	[38,41,45]

Given that environmental pollution with heavy metals most often occurs in the form of complex mixtures [46], it is important to evaluate the total pollution level of all considered heavy metals for a particular sample/site. Two widely used and well-documented integrated indices were used in the present study: pollution load index (PLI) which integrates CFs in the formula/calculation (Table 2), and the potential ecological risk (RI) which takes into account the toxic response factor (Tr) [38] for each considered element (Table 2). The PLI provides an overall measure of pollution by assessing the level of contamination of

multiple heavy metals at a given sample/site [12]. It reflects the extent of contamination and the pollution status of the site, without taking into account the toxicity of the metals.

Another integrated index, RI, is used to evaluate the potential ecological risk posed by HMs in a given sample/site, by considering the concentrations of all metals in combination with their toxicity [7,38]. In this way, an indication of ecological risk and potential threat to the soil/sediment ecosystem and living organisms by heavy metals is specified.

2.4. Statistical Analysis Methods

The Statistica 10.0 program was utilized for all statistical analyses. Before statistical analysis, the database was tested to determine if it presented a normal distribution by using Kolmogorov–Smirnov test. The normal distribution is seen in most of the parameters, thus showing a probability distribution that is symmetrically centered around the average value, indicating that values are more frequently found closer to the mean values.

Descriptive statistics were conducted to present minimum, maximum, and average values to summarize and describe the main features of a data set and determine possible contamination. The standard deviation shows the dispersion of data points around the average value. Skewness quantifies the horizontal gap between the mode (the value that occurs most frequently in the data) and the average (the central tendency of distribution), reflecting asymmetry in the data. In real-world situations, data typically is not normally distributed; instead, it tends to be skewed either to the right (positively skewed) or the left (negatively skewed) [47]. Furthermore, frequency tables provide a clear overview of the distribution of microelements and heavy metal concentrations across the deep sediment samples, helping to identify underlying trends, distributions, and relationships within the data.

Pearson's correlations were conducted to test the relationships between every two parameters in the database. Furthermore, Multivariate Exploratory Techniques were used to visually present the correlations through Principal Components Analysis (PCA) [30,46]. PCA transforms the chosen variables in this study into a new set of dimensions through orthogonal transformation, capturing a majority of the variance. PCA generates principal components equal to the number of original variables, with the selection of those determined by their Eigenvalues > 1. The resulting graph can be used to assess the correlations between variables through factor loadings [22,48,49]. For the cumulative variance of the principal components of less than 70% in PCA, the data set is not adequately represented by the chosen components. In such cases, it may be beneficial to reduce the number of parameters considered by focusing on factor loadings, which show the contribution of each original variable to the principal components. This approach helps to identify key variables and improve data representation.

3. Results and Discussion

3.1. Overview of the Chemical Composition of Dry Samples

The analysis of the dry matter composition shows that SiO_2 and Al_2O_3 are the dominant components, as the deep sediments were rich in clay minerals (Tables 3 and A2). Various geochemical and hydrological processes influence the behavior of metals in soils. These processes are affected by soil and sediment mineralogy, texture, organic matter content, and human activities [50]. Key processes contributing to trace element retention in soils include inorganic and organic complexation, precipitation, adsorption, and the formation of mixed oxides. These interactions play a crucial role in determining the availability and mobility of metals within the soil and sediment environment [51]. The overview of the results on microelement composition (Table 4) shows the maximum allowable concentrations (MAC) according to national regulations for agricultural land and soil [52–54]. The national regulations were used in this study [54] with an established list of target and remediation threshold values to assess potential contamination. These values closely align with the Dutch guidelines for soil remediation [55].

Table 3. Descriptive statistics overview of oxide content (%) and associated parameters (RS, CCC, and layer thickness).

	SiO_2	Al_2O_3	Fe_2O_3	CaO	MgO	Na_2O	K_2O	P_2O_5	SO_3	TiO_2	RS [1]	CCC	TOC	Layer Thickness (m)
Minimum	60.93	15.99	0.86	0.06	1.02	0.17	1.87	0.03	0.01	0.18	0.96	0.00	0.00	0.30
Maximum	79.19	28.11	6.65	1.21	3.88	0.98	4.56	0.29	0.08	0.37	58.52	1.20	1.20	3.00
Average	69.58	23.30	1.77	0.21	1.53	0.32	3.24	0.07	0.02	0.27	22.97	0.03	0.03	1.68
StDev [1]	2.28	1.68	0.81	0.10	0.29	0.10	0.40	0.04	0.01	0.03	9.93	0.12	0.12	0.51
Skewness	0.10	−0.20	2.90	5.20	5.50	2.4	0.10	2.90	2.3	0.20	0.20	5.80	1.0	−0.50
Median	69.64	23.23	1.51	0.20	1.51	0.30	3.24	0.06	0.01	0.27	23.27	0.00	0.10	1.85

[1] StDev—Standard deviation; RS—Remains on the 0.063 mm sieve; CCC—Total contents of carbonates; TOC—Total organic carbon.

Table 4. Descriptive statistics of selected microelements (µg/g) in the analyzed deep sediment samples.

	As	Ba	Cd	Co	Cr	Cu	Hg	Ni	Pb	Sb	Se	Tl	V	Zn
Minimum	0.90	40.00	0.10	0.50	51.90	7.00	0.10	13.10	0.15	0.20	0.10	0.80	58.30	21.20
Maximum	22.00	995.00	1.60	44.93	150.30	37.00	1.20	155.30	39.40	4.90	0.75	2.50	177.50	224.30
Average	4.02	525.64	0.28	4.64	78.63	18.11	0.11	31.41	21.69	1.61	0.41	1.34	107.03	74.38
StDev *	2.83	113.22	0.33	7.61	11.90	5.26	0.08	11.62	5.11	1.19	0.16	0.27	18.66	31.68
MAC agric [48]	25	/	3	/	100	100	2.00	50	100	/	/	/	/	300
MAC soil [52,54]	29	160	0.8	9	100	36	0.30	35	85	3	0.7	1	42	140
Remediation value [52,54]	55	625	12	240	380	190	10.00	210	530	15	100	15	250	720
Hammam et al., 2022 [49]	/	/	0.88	28.62	82.63	51.57	/	/	31.54	/	/	/	/	93.91
Skewness	3.70	0.90	2.00	2.30	1.50	0.30	11.7	5.10	0.20	0.40	−1.20	1.10	0.70	1.10
Median	3.40	502.9	0.10	0.50	76.55	18.05	0.10	30.25	21.30	1.45	0.50	1.30	105.65	69.95

* StDev—Standard deviation; MAC agric.—Maximum allowable concentration in agricultural land; MAC soil—Maximum allowable concentration in soil.

Mercury was mainly found in the samples in low quantity. The allowable limit for mercury is 2 μg/g in agricultural land and 0.3 μg/g in land. Also, the remediation limit value is set to 10 μg/g [52]. Molybdenum was not detected in most of the samples, and where found, the conditions for a level of below 3 μg/g were met. Tin was detected in a low range of 0.2–7.6 μg/g. Since there is only a remediation value of 900 μg/g set in Serbia, tin is excluded from further analysis. The concentration range for silver of 0.1–2.2 μg/g was detected in the samples, and the only limit is the remediation level set at 15 μg/g [54], and so it was not further analyzed.

The concentration of vanadium was found above the limit for soil in all the samples. Most of the samples exceeded the maximum allowable concentrations for barium and thallium. Concentrations of nickel and antimony exceeded the permitted values in approximately 13% of the results, while cadmium exceeded the allowed values in 12% of the cases. Cobalt and chromium were found within permitted values in about 6% of the samples. Additionally, a smaller number of samples showed increased shares of copper, zinc, and selenium.

The average concentrations of As, Cd, Co, Cr, Cu, Ni, and Pb are significantly lower than in the agricultural land in Southwestern Serbia, while the concentration of Zn is higher [56]. The average concentration of As, Cd, Co, Cu, Ni, Pb, Sb, and Zn detected in these samples was well below the values found in the world and Serbia [18,23]. The elevated concentrations of Ni, Cr, and Co in some of the samples are proved to be of a geological influence and/or their retention by the clay layer in the Kolubara district [18,25]. A somewhat increased share of Zn in some of the samples may be considered of anthropogenic origin [18].

Compared to the global average for topsoils, the analyzed samples exhibited lower concentrations of As, Co, Mo, and Ni, while showing an increased concentration of Cd and Se in some of the samples [57]. A selenium deficiency, known to exist in Serbian topsoils, was also detected at lower sediment levels [58]. Since the concentrations of Cd, Pb, and Zn are not highly elevated, it is seen that this region is not under the hydrogeological influence of the previous Pb-Zn mine in this area (Veliki Majdan) [18,58]. In this region, the average concentration of Zn is higher than the background value [18]. Additionally, the detected shares of manganese (Mn) and copper (Cu) were not increased and were found to be unaffected by the antimony (Sb) mine in Stolice [16], Figure 1. However, the increased concentration of Sb, Hg, and Zn may have been partially caused by the tailing's spillage in 2014 [59]. Compared to the element concentrations reported by Hammam et al. (2022) [49], the mean concentrations of Cd, Co, Cr, Cu, Pb, and Zn in this study were significantly lower, especially in the cases of Cd, Co, and Cu.

RS was the parameter that showed the presence of sand in the deep sediments, and its value was around 23% on average. The samples occasionally contained total calcium and magnesium carbonates (CCC). LOI varied from 2.40 to 11.54% (4.91% on average) and depended almost only on the content of clay minerals, as seen before [27]. Most of the samples contained very low TOC. The variation in the concentration of organic matter in deep sediment layers is the result of a complex interplay between the deposition environment, sedimentation rate, organic matter sources, redox conditions, and long-term diagenetic processes. In areas with high biological productivity, rapid sedimentation, and anoxic conditions, TOC concentrations are typically higher. Conversely, like in the studied samples, in environments where organic material decomposes more rapidly (due to oxygen exposure, low productivity, or slow burial), TOC concentrations are lower.

In Table 3, skewness values for most oxides were positive in the range from 0.10 (K_2O) to 5.50 (MgO). Their median concentrations for most parameters (Table 3) were slightly lower than the average but generally comparable, indicating an approximately symmetrical distribution. The negative skewness values were obtained for Al_2O_3 (−0.20) and layer thickness (−0.50). Although the distribution of Al_2O_3 exhibits negative skewness (and an asymmetric distribution is expected), the proximity of the average (23.30) and

median (23.23) indicates that the skewness is mild and does not significantly affect the central tendency.

The skewness values of elements listed in Table 4 were generally positive, ranging from 0.20 (Pb) to 11.7 (Hg), except for Se, which exhibited a negative skewness of −1.20. This suggests that, for most elements, the average concentrations are typically lower than the median. For elements such as Ba, Cr, Cu, Ni, Pb, Tl, V, and Zn, the small difference between the median and average values indicates a nearly symmetrical distribution. In contrast, Se showed a higher median than average, suggesting a distribution with a greater number of higher concentrations and a few exceptionally low values that lower the mean, resulting in a negatively skewed distribution. The observed distribution patterns for these elements are consistent with natural variability, and the presence of heavy metals with symmetrical distributions can often be attributed to natural sources [60].

The soil protection policy in Serbia is implemented by the Ministry of Environmental Protection, with the help of the administration for waste management and soil conservation, under EU and national legislation concerning laws on environmental protection, land, agricultural lands protection, and waste management. The emphasis in the Republic of Serbia is on agricultural land protection, while the monitoring of deep sediment layers is neglected.

3.2. Vertical and Spatial Distributions of Elements in the Deep Sediment Profiles

The histograms illustrating the vertical and spatial distributions of elements contributing most significantly to deep sediment layer contamination are presented in Figure 2. Tl, V, and Ba are found above MAC values in most samples.

Thallium is a highly toxic element that the US EPA has designated a priority pollutant [61]. Major human-made sources of Tl include coal combustion, mining and smelting activities, and cement production. Due to the volatility of Tl compounds at high temperatures, they are not effectively captured by emission control systems, leading to a significant release into the ecosystem. Minerals such as illite clays play a crucial role in immobilizing Tl in soils [62]. The analyzed samples indicated Tl concentrations consistent with slope-wash rocks and alluvial deposits downstream [63], surpassing the MAC limits for soil [52–54]. Most samples contained over 1 μg/g of Tl (Figure 2a,b).

Vanadium is one of the most commonly found trace elements in nature [64]. Most samples contained 80–120 μg/g of vanadium, which is two to three times higher than the allowable limit in the land (Table 5, Figure 2c,d). The highest concentrations of V were observed in sediment layers at depths of 20–40 m. These elevated cases were not found in boreholes BC-14, BC-18, BC-24, BC-24, and BC-26, but were seen in most of the other boreholes. The appearance of V was followed by the distribution of RS in the boreholes, which mostly ranged from 10 to 30% (results not presented). While high concentrations of V may originate from human activities, in this case, its occurrence is more closely related to the parent clay sedimentary rock (argillaceous sediments) [64].

Barium is the fourteenth most common element on Earth and is characterized by low mobility in soil. Ba is strongly bound to the particles of clay minerals. However, there has been limited research on the presence of barium in soil [65]. The highest concentrations of Ba found ranged from 440 to 500 μg/g, which exceeds the allowable limit for land use (Tables 4 and 5, Figure 2e,f). These elevated cases were primarily observed in boreholes BC-16 and BC-27 at depths of up to 40 m.

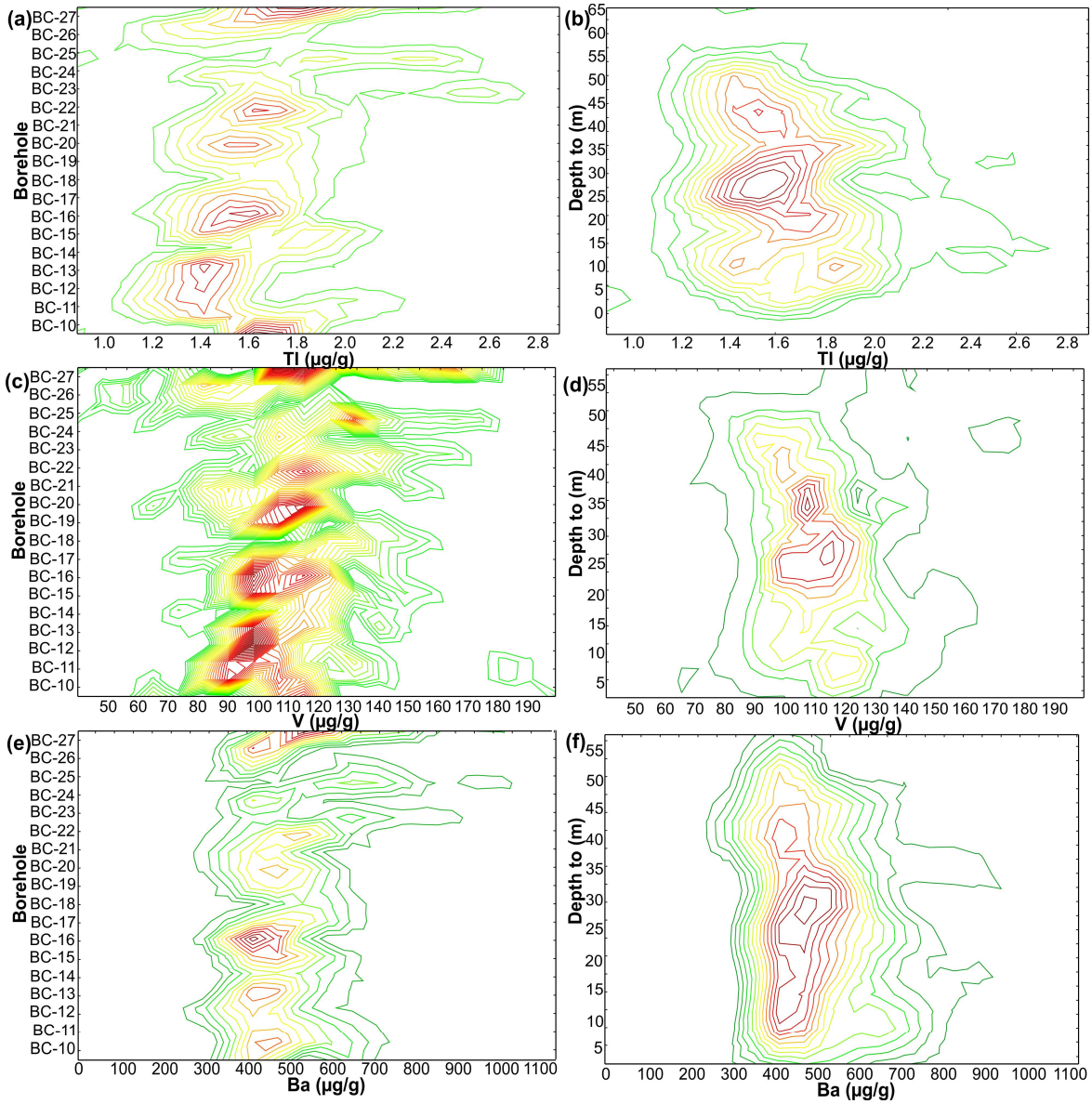

Figure 2. Bivariate histograms of Tl (**a**,**b**), V (**c**,**d**), and Ba (**e**,**f**) distributions through boreholes and depths of sampling (the color shades vary from the palest yellow to the darkest red as the concentrations of the elements increase).

Table 5. Frequencies of the microelements' contents that exceed national MACs.

	V	Cr	Co	Ni	Cu	As	Se	Cd	Sb	Pb	Tl	Zn		Ba	
Sort (μg/g)	**%**	**%**	**%**	**%**	**%**	**%**	**%**	**%**	**%**	**%**	**%**	**Sort (μg/g)**	**%**	**Sort (μg/g)**	**%**
0–20	0.4	0.4	93.8	10.2	64.4	98.0	99.2	99.2	99.2	40.2	100.0	0–50	21.5	0–200	1.6
20–40	0.0	0.0	4.7	75.0	34.8	1.2	0.0	0.0	0.0	59.0	/	50–100	59.8	200–400	5.9
40–60	0.8	4.3	0.8	13.3	0.0	0.0	0.0	0.0	0.0	0.0	/	100–150	15.6	400–600	71.1
60–80	3.9	55.8	0.0	0.0	0.0	0.0	0.0	0.0	0.0	0.0	/	150–200	2.0	600–800	18.0
80–100	31.6	34.0	0.0	0.0	0.0	0.0	0.0	0.0	0.0	0.0	/	200–250	0.8	800–1000	3.1
100–120	44.1	3.5	0.4	0.4	0.4	0.4	0.4	0.4	0.4	0.4	/	/	/	/	/
120–140	13.3	0.8	0.0	0.0	0.0	/	/	/	/	/	/	/	/	/	/
140–160	3.9	0.8	0.0	0.8	0.0	/	/	/	/	/	/	/	/	/	/
160–180	1.6	/	/	/	/	/	/	/	/	/	/	/	/	/	/

3.3. Contribution of Metals to the Contamination of Soil

The enrichment factor (EF) was used to describe the enrichment level of particular HMs in deep sediment profiles and its potential anthropogenic influence (Table 6, Figure 3). The calculation of the EF involved the normalization of HM concentrations using Mn as a reference element [40], based on the assumption that its natural abundance in the Earth's crust remains unaffected by anthropogenic influences, while geochemical baseline values reported in [39] were used as the background concentrations of elements.

Table 6. Descriptive statistics of the enrichment factor for heavy metals.

EF	As	Cd	Cr	Cu	Hg	Ni	Pb	Zn
Minimum	1.85	0.71	0.83	0.46	1.07	0.40	0.20	0.67
Maximum	212.7	152.1	39.7	15.3	247.4	39.7	111.3	61.4
Average	36.3	21.7	13.2	5.42	22.6	6.95	29.1	17.7

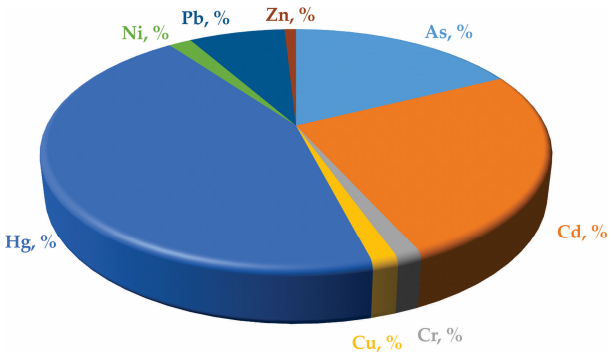

Figure 3. The average contribution of heavy metals to the potential ecological risk.

The associated enrichment levels were as follows: Pb (0.20–111.3), low to extremely high; Ni (0.40–39.7), low to very high; Cu (0.46–15.3), low to significant; Zn (0.67–61.4), low to extremely high; Cd (0.71–152.1), low to extremely high; Cr (0.83–39.7), low to very high; Hg (1.07–247.4), low to extremely high; and As (1.85–212.7), low to extremely high enrichment. The average EF values for the studied HMs (Figure 3) showed the following descending order: As (36.3) > Pb (29.1) > Hg (22.6) > Cd (21.7) > Zn (17.7) > Cr (13.2) > Ni (6.95) > Cu (5.42). According to the classification criteria established in the literature [42,43], the average values indicate that the analyzed sediment profiles show a very high enrichment of As, Pb, Hg, and Cd, along with significant enrichment of Ni, Cr, Zn, and Cu. It is important to note that, although the measured concentrations of As, Pb, Hg, and Cd were below the MACs, their EF values revealed high levels of enrichment. The findings suggest that EF values for As, Pb, Hg, and Cd show notable enrichment, likely resulting from localized or historical inputs. These may be due to anthropogenic activities or reflect geochemical anomalies with specific regional distribution patterns linked to the composition of the parent rock. While the absolute concentrations of these elements remain within regulatory limits, their enrichment values (EF values) may signal potential long-term risks, especially in the conditions of changing land use patterns. This suggests that their concentrations may be elevated relative to their geochemical baseline levels and/or the natural abundance of Mn in the studied environment; (as the enrichment factor was used to assess deviations from natural background levels, normalized against a reference element). Therefore, while these elements may be locally enriched, this does not necessarily indicate an immediate ecological danger. Likewise, the development of mining activities in this region could worsen contamination by disturbing the soil and redistributing these elements. Therefore, even if the current anthropogenic contribution is not apparent in the analyzed deep sediment of this rural area with minimal anthropogenic impact, the observed enrichment levels of As, Pb, Hg, and Cd, which significantly exceed the threshold

in some of the deep sediment layers tested, suggest potential risks, especially in areas prone to significant land use changes.

The highest EF values, categorized as extremely high enrichment, were obtained individually for Hg > As > Cd > Pb > Zn, which follows the order of boreholes: BC-20 (34.0–36.0 m) > BC-25 (30.0–31.8 m) > BC-14 (14.0–15.0 m) > BC-11 (49.0–51.2 m) > BC-14 (22.4–23.0 m), respectively.

The highest EF values for Ni, Cr, and Cu, classified as significant enrichment, were recorded in the following boreholes: BC-14 (22.4–24.5 m), BC-11 (49.0–51.2 m), and BC-22 (34.0–35.8). Overall, borehole BC-14 (22.4–23.0 m) demonstrated enrichment in Ni and Zn, with their concentrations reaching peak levels at the locations, while in sample BC-11 (49.0–51.2 m) the highest enrichment levels for Cr and Pb were recorded.

All elements at boreholes BC-27 and BC-20 showed EF values below 2, indicating deficiency or minimal enrichment. Considering the intended land use of the borehole sites BC-20 (meadow, class VI) and BC-27 (agricultural field, class VI), where the lowest EF values are consistently observed in the deep layers, it can be inferred that anthropogenic activities have had minimal impact on the deeper sediment strata. Specifically, the lowest EF values for Cr and Hg were recorded at BC-27 (50.0–52 m), for Cd at BC-27 (48.0–50.0 m), and for As, Ni, and Zn at BC-27 (41.0–43.6 m). Pb exhibited minimal enrichment at BC-20 (34.0–36.0 m), unlike the other elements.

3.4. Environmental Pollution Status of HMs in the Deep Sediment Profiles

The pollution load index (PLI) represents the geometric mean of the contamination factors (CF) (Tables 2 and A3) calculated for different trace metals and serves as a useful tool to assess the overall level of pollution associated with the presence of potentially toxic HMs in the samples [41]. Furthermore, the PLI provides the contamination status of deep sediment assessments by integrating the contributions of all considered elements (As, Cd, Cr, Cu, Hg, Ni, Pb, Zn) [12].

The results of PLI for each sample are presented in Table A3. The PLI values ranged from 0.90 at BC-27 (Sample 245, 37.0–39.0 m) to 1.81 at BC-14 (Sample 74, 19.40–21.1 m). These values indicate that the status of the sediment samples varied from no contamination (PLI < 1) to high contamination (PLI > 1). The average PLI value was 0.80, indicating baseline contamination. This suggests that there is no serious pollution in the studied samples. The majority of the analyzed samples (73.6%) were classified as having baseline pollution (0 < PLI < 1), with values fluctuating around 1, implying no considerable input from anthropogenic sources. This suggests a relatively healthy ecological status concerning heavy metal pollution. Additionally, no samples exhibited zero (PLI = 0), while 26.4% of the samples showed high levels of pollution (PLI > 1).

The potential ecological risk index (RI), introduced by Håkanson [38], serves as a comprehensive measure for quantifying the sensitivity of soil or sediment ecosystems [30,51]. This index highlights the link between heavy metal content, source, and the associated risk [66]. The calculated RI values ranged from 81.1 (BC-27) to 752.2 (BC-20), (Table A3), indicating low to very high ecological risk in the studied area, according to the RI classification criteria [38]. The average RI value was 133.5, reflecting a moderate ecological risk level for the analyzed soil. The proportions of RI across different classes were as follows: class I (low risk) accounted for 38%, class II (moderate risk) represented 59.2%, class III (considerable risk) constituted 2.40%, and class IV (very high) comprised 0.40%. The highest RI value was observed in the sample at BC-20 (34.0–36.0 m). This RI value was consistent with the vertical distribution of Hg content in that sample, where it exhibited its highest value (1.20). It should also be noted that Hg, Cd, and As made the most significant contributions to the total RI value, accounting for 43.9%, 25.5%, and 17.7%, respectively (Figure 3). This is attributed to the high ecotoxicity response factors of Hg and Cd, resulting in the considerable contamination of the sample with these metals. Such findings imply that the potential ecological risks from different sources vary in their contribution to deep sediment contamination. This relationship is influenced not only by the concentrations of

heavy metals in the deep sediment but also by the specific properties of these metals, such as the high bioavailability and toxicity of Cd and Hg [66].

3.5. Statistical Analysis Results

The database containing 250 samples, which included the concentration of 11 oxides, 21 elements, and 6 additional variables, was challenging to analyze. The deep sediment samples consisted primarily of quartz and clay minerals, with the dominant share being SiO_2 and Al_2O_3. Hence, the probability and 3D scatter plots of the selected variables indicated that the increased amount remaining on the 0.063 mm sieve was associated with higher levels of SiO_2 in quartz and lower LOI and TOC (Figure 4), which is also seen by Pearson's correlation analysis. Simultaneously, the proportion of Al_2O_3 was lower. Consequently, a higher quantity of quartz led a to reduced loss in ignition, along with lower TOC and clay mineral content [27].

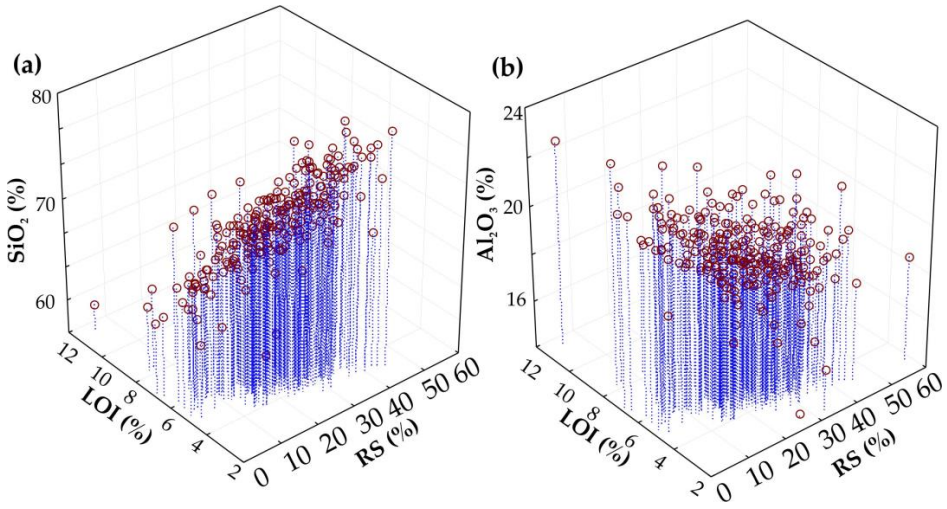

Figure 4. Three-dimensional scatterplots for the selected variables: (**a**) LOI, RS, and SiO_2, (**b**) LOI, RS, and Al_2O_3 (LOI—loss on ignition at 1000 °C, RS—remains on the 0.063 mm sieve).

Spearman's correlation table is not presented due to the huge database, only the most significant data are explained and presented by using the PCA. The results revealed the most intensive *r* for statistically significant relations between the pairs SiO_2/Al_2O_3 and SiO_2/LOI (negative correlations). The next in line by the relevance are positive correlations in pairs Ba/Th, Ba/Pb, La/Ce, U/V, and Zn/Ni. Cluster analysis showed that all the studied parameters were related, while the most significant (grouping ones) were SiO_2 and Ba. Including all the observed parameters in PCA yielded only about 50% of the system description. Thus, a specific statistical methodology consisting of choosing the option to find the maximum likelihood factors was employed to reveal the most significant parameters for further analysis by the PCA. Based on this analysis, the most intensive and statistically significant variability of the parameters was found in the cases listed in Table 7 in descending order (SiO_2, V, Ba, Cr, Pb, Th, Tl, and Al_2O_3).

Table 7. Factor analysis and the highest factor loadings.

	SiO_2	V	Ba	Cr	Pb	Th	Tl	Al_2O_3
Loadings	0.78	−0.84	−0.73	−0.72	−0.72	−0.72	−0.70	−0.55

The PCA based on the selected parameters revealed that the first two factors (Factor 1—60.74% and Factor 2—15.45%) are sufficient to describe the database while explaining 76.2% of the system variability (Figure 5a), with Eigenvalues above 1 [30,49,67]. The mutual proximity of the vectors representing the variables (Figure 5b) indicates that, for

example, Th, Tl, and Ba, and then also Pb, Cr, and V concentrations are highly related due to their statistically significant and positive correlations. This shows that the geochemistry of these elements in parent material and deep sediments is similar [58]. In addition, all these elements are positively correlated to Al_2O_3 and negatively correlated to SiO_2, indicating their presence within the clayey fraction, and their absence from the coarse fraction represented by SiO_2 in quartz. This shows that the intergranular porosity nature of the sediments in this area is highly influential [68].

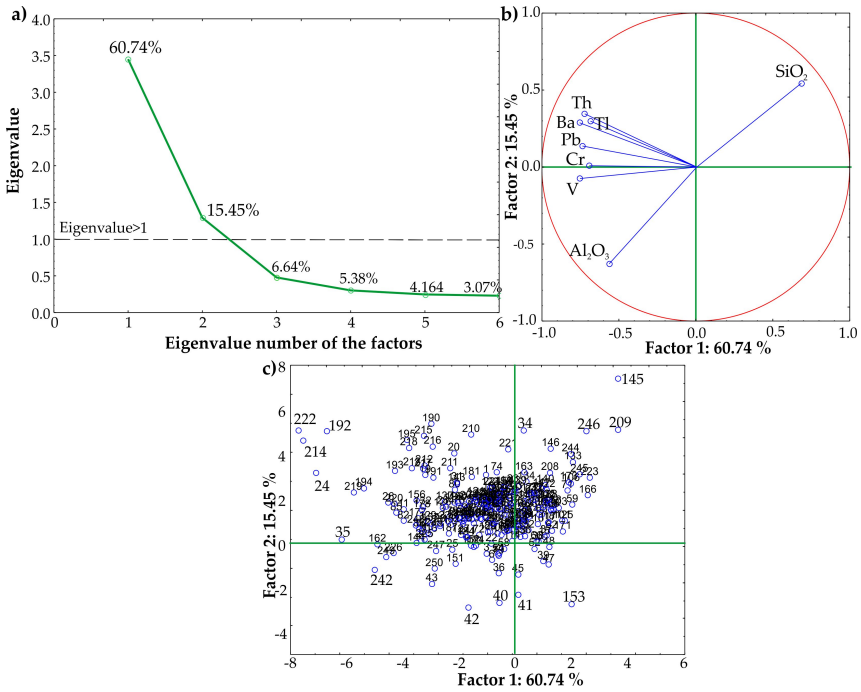

Figure 5. (**a**) Eigenvalues of the factors, (**b**) PCA of the most influential and selected parameters and (**c**) projection of the cases on the factor plane (samples number 1–250).

When the samples are projected on the factor plane (Figure 5c), most are seen as similar standing in a cloud, but some stand out. While parallelly observing Figure 5b,c, it is seen that the samples with the highest concentrations of Al_2O_3 are seen in BC-20 (11.6–13.2 m, sample number 145). The samples with the highest shares of Th, Tl, and Ba are found in BC-23 (at 17.0–19.0 m, sample number 192), and BC-25 (19.7–22.0 m and 44.0–46.5 m, sample numbers 214 and 222), while the highest content of V is found in borehole BC-11 (49.0–51.2 m, sample number 35).

4. Conclusions

This study investigated the content and vertical distribution of oxides and elements in the deep sediment layers in the rural areas of western Serbia. The 250 samples from a depth of 5–58.5 m were examined using the XRF technique. The deep sediment cores were tested for contamination on a global scale for the first time. Despite the area being relatively distant from heavy traffic and industry, elevated contents of Tl, V, and Ba are observed, mainly originating from the parent material or rock-forming processes that influence the soil's mineralogical and elemental composition. Sporadic elevated concentrations of some elements may be a consequence of the natural deposition, which appears to be the main factor that affects their vertical distribution. Namely, one of the factors influencing the distribution of elements is associated with the hydrogeological characteristics of the studied area, including the transport of elements via water and their retention within clay layers. Once deposited, elements can remain stable, providing evidence that traces the history of past contamination. These results can serve as a baseline assessment for the future monitoring of deep sediment layer quality in this region.

By providing a baseline assessment of element and oxide content in a rural area, this study offers valuable data for future environmental monitoring. Therefore, it highlights the importance of establishing geo-environmental data on elemental levels before mining activities possibly commence in nearby areas. This information can serve as a reference for comparison if contamination occurs at this or surrounding locations. Furthermore, it can serve as a reference for a relatively pristine environment, providing a benchmark for assessing the impact of potential contamination. The results may also be valuable for future deep sediment monitoring worldwide, as this study is the first of its kind.

In summary, deep sediment layer monitoring for heavy metals is essential to assess environmental changes over time and determine historical contamination. Regulations and laws should be established to govern the examination and monitoring of microelements and other important parameters in deep sediments as well.

Author Contributions: Conceptualization, M.R. and M.V.V.; methodology, N.M., M.R. and M.V.V.; software, M.V.V.; validation, N.M.; formal analysis, N.M. and M.V.V.; investigation, N.M., M.R. and M.V.V.; resources, N.M. and M.V.V.; writing—original draft preparation, N.M., M.R. and M.V.V.; writing—review and editing, N.M., M.R., M.V.V. and P.M.V.; visualization, M.V.V. All authors have read and agreed to the published version of the manuscript.

Funding: This research was funded by the Ministry of Science, Technological Development and Innovation of the Republic of Serbia, grant numbers 451-03-66/2024-03/200012 and 451-03-66/2024-03/200287. The APC was funded by Milica (Vidak) Vasić.

Data Availability Statement: Public data are not available. The data may be provided individually at request.

Conflicts of Interest: The authors declare no conflicts of interest. The funder had no role in the design of the study; in the collection, analysis, or interpretation of data; in the writing of the manuscript; or in the decision to publish the results.

Appendix A

Table A1. List of sampling sites (boreholes) and their coordinates.

Boreholes	Latitude (N)	Longitude (E)	Altitude (m)
BC-01	44°25′56.05″	19°39′1.52″	202.12
BC-02	44°25′44.34″	19°39′0.21″	204.14
BC-03	44°25′35.58″	19°38′45.84″	225.43
BC-04	44°25′33.98″	19°38′40.06″	225.67
BC-05	44°25′39.04″	19°38′48.26″	242.59
BC-06	44°25′37.88″	19°38′40.93″	241.17
BC-07	44°25′42.60″	19°38′40.18″	250.44
BC-08	44°25′49.09″	19°38′29.81″	219.01
BC-09	44°25′38.54″	19°38′36.34″	239.12
BC-10	44°25′32.39″	19°38′48.58″	224.58
BC-11	44°25′33.31″	19°38′46.74″	225.73
BC-12	44°25′34.24″	19°38′44.90″	229.83
BC-13	44°25′35.16″	19°38′43.06″	234.03
BC-14	44°25′32.31″	19°38′52.80″	214.51
BC-15	44°25′33.82″	19°38′49.58″	224.34
BC-16	44°25′34.70″	19°38′47.71″	228.19
BC-17	44°25′36.46″	19°38′43.96″	230.78
BC-18	44°25′33.74″	19°38′53.80″	219.85
BC-19	44°25′35.25″	19°38′50.58″	230.41
BC-20	44°25′36.13″	19°38′48.71″	235.38
BC-21	44°25′37.01″	19°38′46.84″	235.68
BC-22	44°25′37.89″	19°38′44.97″	230.07
BC-23	44°25′39.28″	19°38′42.00″	237.02
BC-24	44°25′35.93″	19°38′55.33″	216.06
BC-25	44°25′37.37″	19°38′52.06″	233.81
BC-26	44°25′40.61″	19°38′44.70″	243.25
BC-27	44°25′32.25″	19°38′43.51″	225.48

Table A2. Frequencies of the oxides' contents and other properties.

SiO_2		Al_2O_3		Fe_2O_3		CaO		MgO		Na_2O		K_2O		TiO_2		SO_3	
Group (%)	**%**	**Group (%)**	**%**	**Group (%)**	**%**	**Group (%)**	**%**	**Group (%)**	**%**	**Group (%)**	**%**	**Group (%)**	**%**	**Group (%)**	**%**	**Group (%)**	**%**
60–70	60.8	16–20	2.8	0.8–1.5	8.8	0.0–0.5	98.8	1.0–1.5	45.6	0.0–0.5	95.2	1.8–3.0	28.8	0.1–0.2	2.0	0.00–0.02	71.6
70–80	39.2	20–25	81.2	1.5–3.0	84.8	0.5–1.0	1.2	1.5–2.0	52.8	0.5–1.0	4.8	3.0–4.0	66.8	0.2–0.3	84.8	0.02–0.04	21.6
		25–28	16.0	3.0–6.6	6.4			2.0–3.9	1.6			4.0–4.6	4.4	0.3–0.4	13.2	0.04–0.08	6.8

RS		CCC		TOC	
Group (%)	%	Group (%)	%	Group (%)	%
0.0–20.0	40.4	0.0–0.6	99.6	0.00–0.02	92.8
20.0–40.0	50.2	0.6–1.2	0.4	0.02–0.04	7.2
40.0–60.0	9.4				

Table A3. Contamination factor (CF), pollution load index (PLI) and potential ecological risk index (RI) in deep sediment profiles.

Sample	Borehole	CF_{As}	CF_{Cd}	CF_{Cr}	CF_{Cu}	CF_{Hg}	CF_{Ni}	CF_{Pb}	CF_{Zn}	PLI	RI
S1	BC-10	1.06	0.50	0.83	0.25	1.25	0.46	1.81	0.77	0.74	90.6
S2	BC-10	0.83	0.50	0.80	0.27	1.25	0.48	1.55	1.03	0.74	87.5
S3	BC-10	6.33	1.75	0.72	0.43	1.25	0.57	1.90	1.53	1.28	183.3
S4	BC-10	3.00	0.50	0.94	0.32	1.25	0.60	1.97	1.31	0.98	112.6
S5	BC-10	2.97	1.25	0.83	0.16	1.25	0.50	1.49	0.87	0.89	130.5
S6	BC-10	2.39	0.50	0.72	0.31	1.25	0.56	1.78	1.12	0.88	262.0
S7	BC-10	2.00	1.75	0.86	0.36	1.25	0.59	1.94	1.70	1.13	140.3
S8	BC-10	2.33	2.00	0.95	0.42	1.25	0.57	2.42	1.88	1.25	154.1
S9	BC-10	1.56	0.50	0.64	0.23	1.25	0.44	1.49	0.80	0.72	93.4
S10	BC-10	1.67	0.50	0.91	0.45	1.25	0.51	2.29	0.75	0.88	100.5
S11	BC-10	2.33	0.50	0.91	0.43	1.25	0.57	2.62	1.06	0.99	109.3
S12	BC-10	1.67	0.50	0.65	0.23	1.25	0.32	1.89	0.79	0.72	95.9
S13	BC-10	1.94	0.50	0.88	0.27	1.25	0.61	1.96	0.92	0.87	101.3
S14	BC-10	5.28	0.50	0.87	0.23	1.25	0.62	1.73	1.92	1.04	134.3
S15	BC-11	1.94	1.75	0.60	0.25	1.25	0.30	1.34	0.72	0.81	133.3
S16	BC-11	1.83	0.50	0.60	0.24	1.25	0.30	1.44	0.75	0.69	95.1
S17	BC-11	1.22	0.50	0.83	0.29	1.25	0.50	1.65	1.03	0.79	92.1
S18	BC-11	1.22	0.50	0.64	0.32	1.25	0.26	1.34	0.70	0.66	88.8
S19	BC-11	3.17	2.00	0.91	0.37	1.25	0.53	2.27	1.43	1.21	160.8
S20	BC-11	2.61	0.50	0.89	0.30	1.25	0.53	1.94	1.18	0.93	107.9
S21	BC-11	1.44	1.50	0.75	0.36	1.25	0.33	1.75	0.67	0.85	123.8
S22	BC-11	1.39	0.50	0.73	0.36	1.25	0.36	1.61	1.04	0.78	93.0
S23	BC-11	1.22	0.50	0.88	0.21	1.25	0.43	1.40	0.56	0.68	89.7
S24	BC-11	3.72	0.50	1.02	0.54	1.25	0.68	2.93	1.96	1.22	127.0
S25	BC-11	2.06	0.50	0.79	0.45	1.25	0.35	2.22	0.86	0.86	103.1
S26	BC-11	2.78	0.50	1.02	0.30	1.25	0.50	2.33	1.02	0.94	111.4
S27	BC-11	1.89	0.50	0.81	0.21	1.25	0.60	1.77	0.93	0.82	99.3
S28	BC-11	1.78	0.50	0.89	0.13	1.25	0.50	2.14	1.03	0.78	99.4
S29	BC-11	1.50	0.50	0.82	0.17	1.25	0.53	1.83	0.91	0.76	95.2
S30	BC-11	1.67	0.50	0.80	0.18	1.25	0.50	1.70	1.00	0.77	96.2
S31	BC-11	2.00	4.00	0.85	0.17	1.25	0.45	1.82	0.95	1.01	204.9
S32	BC-11	2.78	0.50	0.77	0.13	1.25	0.51	1.61	0.84	0.77	106.4
S33	BC-11	2.61	0.50	0.72	0.25	1.25	0.49	1.58	0.73	0.80	104.9
S34	BC-11	1.56	0.50	0.84	0.18	1.25	0.43	1.56	1.03	0.75	94.1
S35	BC-11	1.06	0.50	1.12	0.42	1.25	0.30	3.15	0.45	0.78	97.6
S36	BC-12	2.39	1.75	0.67	0.32	3.75	0.35	1.52	1.07	1.08	239.7
S37	BC-12	1.72	1.75	0.61	0.35	1.25	0.38	1.57	1.35	0.95	133.8
S38	BC-12	0.89	0.50	0.67	0.30	1.25	0.31	1.18	0.71	0.64	84.9
S39	BC-12	0.94	1.75	0.67	0.31	1.25	0.34	1.16	0.86	0.79	123.2
S40	BC-12	1.56	0.50	0.74	0.35	1.25	0.32	1.31	0.87	0.74	92.8
S41	BC-12	1.78	0.50	0.74	0.33	1.25	0.38	1.22	1.15	0.79	95.0
S42	BC-12	3.11	1.75	0.77	0.16	1.25	0.41	1.74	1.12	0.95	147.8
S43	BC-12	3.39	0.50	0.82	0.25	1.25	0.42	1.90	0.89	0.86	114.3
S44	BC-12	2.44	0.50	0.72	0.23	1.25	0.33	1.70	0.50	0.72	102.7
S45	BC-12	0.67	6.50	0.70	0.18	1.25	0.38	0.98	0.39	0.75	261.2
S46	BC-12	1.39	1.75	0.87	0.43	1.25	0.22	1.30	0.51	0.80	128.3
S47	BC-12	1.17	0.50	0.62	0.24	1.25	0.21	0.89	0.44	0.55	85.0
S48	BC-12	1.00	0.50	0.59	0.24	1.25	0.22	1.33	0.42	0.57	85.6

Table A3. *Cont.*

Sample	Borehole	CF_{As}	CF_{Cd}	CF_{Cr}	CF_{Cu}	CF_{Hg}	CF_{Ni}	CF_{Pb}	CF_{Zn}	PLI	RI
S49	BC-13	1.11	0.50	0.67	0.15	1.25	0.43	1.27	1.13	0.67	87.8
S50	BC-13	1.50	5.00	0.76	0.21	1.25	0.74	2.01	2.23	1.22	233.5
S51	BC-13	3.39	0.50	0.73	0.33	1.25	0.42	1.55	1.70	0.93	113.6
S52	BC-13	2.28	0.50	0.70	0.24	1.25	0.36	1.28	1.00	0.76	99.6
S53	BC-13	1.28	0.50	0.70	0.20	1.25	0.30	1.22	0.74	0.65	88.5
S54	BC-13	1.39	1.75	0.82	0.44	1.25	0.50	1.57	1.27	1.01	131.8
S55	BC-13	11.06	1.75	0.64	0.30	1.25	0.35	1.67	0.51	1.04	226.5
S56	BC-13	0.94	4.50	0.72	0.44	1.25	0.29	1.36	0.62	0.89	206.9
S57	BC-13	1.61	1.75	1.06	0.46	1.25	0.41	2.29	0.78	1.03	137.3
S58	BC-13	1.39	0.50	0.68	0.25	1.25	0.36	1.47	0.54	0.67	91.2
S59	BC-13	0.72	0.50	0.57	0.28	1.25	0.38	1.27	0.47	0.60	83.5
S60	BC-13	1.44	0.50	0.81	0.39	1.25	0.21	1.70	0.61	0.71	93.2
S61	BC-13	1.33	0.50	0.72	0.32	1.25	0.29	1.99	0.50	0.70	93.3
S62	BC-13	1.28	0.50	0.58	0.33	1.25	0.22	1.39	0.54	0.63	91.1
S63	BC-13	1.11	0.50	0.71	0.37	1.25	0.31	1.24	0.70	0.69	252.5
S64	BC-13	1.11	0.50	0.66	0.34	1.25	0.24	1.59	0.54	0.65	131.5
S65	BC-13	2.22	4.50	0.60	0.27	1.25	0.35	2.24	0.49	0.97	105.7
S66	BC-13	1.50	0.50	0.52	0.28	1.25	0.26	2.58	0.57	0.69	109.4
S67	BC-14	1.94	8.00	0.84	0.49	1.25	0.49	2.20	1.46	1.37	165.4
S68	BC-14	2.67	0.50	0.77	0.34	1.25	0.36	1.53	0.86	0.82	104.8
S69	BC-14	1.56	0.50	0.72	0.40	1.25	0.46	1.83	1.46	0.88	107.4
S70	BC-14	2.00	1.75	0.75	0.36	1.25	0.42	1.87	1.44	1.04	88.4
S71	BC-14	1.39	6.50	0.63	0.32	1.25	0.33	1.31	1.00	1.00	106.8
S72	BC-14	3.28	3.50	0.78	0.38	1.25	0.43	1.81	0.99	1.16	146.9
S73	BC-14	2.61	0.50	0.72	0.48	1.25	0.55	2.02	1.81	1.02	206.5
S74	BC-14	4.17	5.00	0.70	0.42	1.25	2.07	2.26	3.20	1.81	111.2
S75	BC-14	2.06	4.50	0.74	0.33	1.25	0.40	1.70	1.13	1.10	130.0
S76	BC-15	1.78	4.00	0.66	0.25	1.25	0.34	1.72	0.75	0.95	180.9
S77	BC-15	2.22	0.50	0.77	0.33	1.25	0.45	1.78	1.42	0.89	89.2
S78	BC-15	1.89	0.50	0.72	0.26	1.25	0.37	1.62	1.16	0.79	104.3
S79	BC-15	1.83	0.50	0.77	0.47	1.25	0.65	1.69	1.63	0.96	92.4
S80	BC-15	1.72	0.50	0.84	0.46	1.25	0.40	2.05	1.12	0.89	109.0
S81	BC-15	2.00	0.50	0.78	0.33	1.25	0.29	1.34	0.82	0.75	125.3
S82	BC-15	2.28	0.50	0.83	0.45	1.25	0.42	2.22	1.31	0.95	83.9
S83	BC-15	3.94	0.50	0.97	0.31	1.25	0.52	1.63	1.39	0.98	92.2
S84	BC-15	2.17	0.50	0.72	0.33	1.25	0.39	1.71	1.15	0.84	99.9
S85	BC-15	3.11	4.00	1.50	0.43	1.25	0.56	1.98	0.74	1.30	109.0
S86	BC-15	3.56	0.50	0.83	0.46	1.25	0.50	2.15	2.12	1.09	104.3
S87	BC-15	2.50	1.75	0.74	0.35	1.25	0.40	2.03	1.41	1.06	93.1
S88	BC-15	2.33	0.50	0.81	0.29	1.25	0.37	2.09	1.04	0.85	91.9
S89	BC-15	1.56	0.50	0.76	0.29	1.25	0.35	1.59	0.72	0.74	94.3
S90	BC-15	2.89	0.50	0.70	0.24	1.25	0.41	1.94	0.89	0.82	752.2
S91	BC-15	3.00	0.50	0.72	0.31	1.25	0.38	2.06	1.10	0.88	93.7
S92	BC-16	3.00	0.50	0.82	0.29	1.25	0.43	1.68	1.19	0.89	211.2
S93	BC-16	1.61	0.50	0.81	0.30	1.25	0.35	1.92	0.88	0.78	116.8
S94	BC-16	1.06	0.50	0.75	0.41	1.25	0.41	1.42	1.20	0.78	97.8
S95	BC-16	1.06	0.50	0.72	0.29	1.25	0.31	1.27	0.74	0.67	128.0
S96	BC-16	2.39	2.00	0.85	0.39	1.25	0.43	1.45	0.91	1.01	511.2
S97	BC-16	1.56	0.50	0.75	0.36	1.25	0.32	1.73	0.96	0.78	232.3
S98	BC-16	2.72	0.50	0.74	0.38	1.25	0.48	1.44	1.48	0.91	92.9
S99	BC-16	2.50	0.50	0.75	0.36	1.25	0.34	1.87	0.86	0.83	120.2
S100	BC-16	2.39	0.50	0.76	0.41	1.25	0.41	1.93	1.16	0.90	98.6

Table A3. *Cont.*

Sample	Borehole	CF_{As}	CF_{Cd}	CF_{Cr}	CF_{Cu}	CF_{Hg}	CF_{Ni}	CF_{Pb}	CF_{Zn}	PLI	RI
S101	BC-16	2.67	1.75	0.83	0.20	1.25	0.29	1.22	0.59	0.82	105.3
S102	BC-16	2.89	0.50	0.72	0.24	1.25	0.35	1.85	0.94	0.81	100.7
S103	BC-16	2.50	0.50	0.70	0.17	1.25	0.32	1.42	0.71	0.70	84.0
S104	BC-16	1.78	0.50	0.76	0.19	1.25	0.33	1.40	0.68	0.69	93.3
S105	BC-16	3.94	0.50	0.79	0.26	1.25	0.38	1.83	0.90	0.87	88.7
S106	BC-16	1.89	0.50	0.67	0.16	1.25	0.28	1.40	0.60	0.65	96.4
S107	BC-16	1.56	0.50	0.74	0.42	1.25	0.26	1.62	0.42	0.69	95.1
S108	BC-16	0.89	0.50	0.75	0.34	1.25	0.23	1.22	0.34	0.58	126.8
S109	BC-16	1.00	0.50	0.75	0.45	1.25	0.25	1.59	0.37	0.65	149.2
S110	BC-16	0.72	4.50	0.87	0.45	1.25	0.23	1.49	0.44	0.83	101.8
S111	BC-17	1.61	0.50	0.70	0.19	1.25	0.36	1.47	1.11	0.73	100.1
S112	BC-17	1.94	0.50	0.75	0.21	1.25	0.38	1.73	1.24	0.79	113.1
S113	BC-17	4.89	1.75	0.83	0.43	1.25	0.45	2.16	1.67	1.25	132.3
S114	BC-17	1.94	0.50	0.73	0.26	1.25	0.38	1.38	1.11	0.78	187.3
S115	BC-17	0.81	2.50	0.74	0.34	1.25	0.33	1.34	0.82	0.83	118.0
S116	BC-17	1.39	0.50	0.72	0.37	1.25	0.40	1.66	0.99	0.79	134.6
S117	BC-17	1.22	0.50	0.69	0.35	1.25	0.37	1.35	1.21	0.76	159.9
S118	BC-17	1.28	1.75	0.82	0.46	1.25	0.44	1.81	2.39	1.09	102.2
S119	BC-17	1.33	4.00	0.75	0.42	1.25	0.34	1.52	0.80	0.99	101.0
S120	BC-17	1.28	0.50	0.76	0.39	1.25	0.26	1.58	0.62	0.70	91.9
S121	BC-17	1.33	0.50	0.87	0.36	1.25	0.25	1.33	0.59	0.69	187.1
S122	BC-17	1.17	1.75	0.64	0.20	1.25	0.24	1.42	0.40	0.68	117.2
S123	BC-17	0.67	0.50	0.78	0.24	1.25	0.23	1.76	0.44	0.59	91.9
S124	BC-17	2.17	0.50	0.74	0.21	1.25	0.24	1.43	0.50	0.66	126.2
S125	BC-17	1.44	0.50	0.60	0.20	1.25	0.26	1.55	0.41	0.60	91.1
S126	BC-18	2.11	5.50	0.76	0.39	1.25	0.32	2.13	0.62	1.08	252.5
S127	BC-18	2.06	1.50	0.77	0.32	1.25	0.41	1.91	1.13	0.98	131.5
S128	BC-18	2.44	0.50	0.73	0.38	1.25	0.36	2.02	1.00	0.86	105.7
S129	BC-18	2.50	0.50	0.86	0.41	1.25	0.45	2.34	1.76	1.00	109.4
S130	BC-18	5.22	1.50	0.73	0.44	1.25	0.64	1.71	2.77	1.33	165.4
S131	BC-18	2.11	0.50	0.77	0.45	1.25	0.42	2.20	1.81	0.97	104.8
S132	BC-18	2.22	0.50	0.81	0.47	1.25	0.38	2.62	1.19	0.94	107.4
S133	BC-19	1.22	0.50	0.66	0.22	1.25	0.32	1.27	0.77	0.66	88.4
S134	BC-19	2.83	0.50	0.66	0.19	1.25	0.37	1.69	0.88	0.77	106.8
S135	BC-19	2.39	2.00	0.69	0.33	1.25	0.35	1.46	0.92	0.94	146.9
S136	BC-19	2.17	4.00	0.74	0.25	1.25	0.47	1.70	1.21	1.09	206.5
S137	BC-19	2.67	0.50	0.85	0.40	1.25	0.67	2.14	1.78	1.05	111.2
S138	BC-19	0.78	2.00	0.70	0.29	1.25	0.31	1.41	0.83	0.78	130.0
S139	BC-19	1.28	3.50	0.76	0.27	1.25	0.33	1.53	0.90	0.92	180.9
S140	BC-19	1.25	0.50	0.70	0.21	1.25	0.29	1.41	0.77	0.66	89.2
S141	BC-19	2.28	0.50	0.79	0.42	1.25	0.50	1.78	1.46	0.94	104.3
S142	BC-19	1.39	0.50	0.72	0.31	1.25	0.34	1.53	1.17	0.76	92.4
S143	BC-19	2.61	0.50	0.84	0.45	1.25	0.53	1.87	1.93	1.02	109.0
S144	BC-19	4.06	0.50	0.90	0.47	1.25	0.63	2.10	1.94	1.14	125.3
S145	BC-20	0.89	0.50	0.58	0.14	1.25	0.29	1.14	1.04	0.59	83.9
S146	BC-20	1.56	0.50	0.71	0.19	1.25	0.33	1.36	0.88	0.69	92.2
S147	BC-20	2.28	0.50	0.72	0.20	1.25	0.37	1.39	0.86	0.74	99.9
S148	BC-20	2.94	0.50	0.73	0.29	1.25	0.42	1.69	1.14	0.86	109.0
S149	BC-20	2.56	0.50	0.69	0.23	1.25	0.41	1.59	1.19	0.82	104.3
S150	BC-20	1.50	0.50	0.76	0.37	1.25	0.29	1.48	0.87	0.75	93.1
S151	BC-20	1.17	0.50	0.80	0.38	1.25	0.38	1.75	1.13	0.80	91.9
S152	BC-20	1.33	0.50	0.89	0.47	1.25	0.59	1.56	1.17	0.88	94.3
S153	BC-20	1.17	4.50	0.72	0.34	15.00	0.32	0.01	0.74	0.70	752.2
S154	BC-20	1.44	0.50	0.75	0.36	1.25	0.38	1.56	1.23	0.80	93.7
S155	BC-20	1.33	4.50	0.76	0.34	1.25	0.26	1.54	0.62	0.91	211.2

Table A3. *Cont.*

Sample	Borehole	CF_{As}	CF_{Cd}	CF_{Cr}	CF_{Cu}	CF_{Hg}	CF_{Ni}	CF_{Pb}	CF_{Zn}	PLI	RI
S156	BC-20	3.33	0.50	0.86	0.41	1.25	0.53	2.14	1.31	1.01	116.8
S157	BC-20	1.67	0.50	1.25	0.34	1.25	0.50	1.70	0.93	0.88	97.8
S158	BC-20	1.33	1.75	0.70	0.27	1.25	0.36	1.37	0.70	0.81	128.0
S159	BC-20	1.14	3.75	0.74	0.30	9.38	0.36	1.34	0.82	1.17	511.2
S160	BC-20	3.22	4.50	0.73	0.26	1.25	0.44	1.86	0.90	1.12	232.3
S161	BC-20	1.67	0.50	0.69	0.27	1.25	0.32	1.24	0.67	0.69	92.9
S162	BC-20	3.44	0.50	0.91	0.30	1.25	0.56	2.54	1.96	1.06	120.2
S163	BC-21	2.11	0.50	0.67	0.21	1.25	0.40	1.38	1.23	0.77	98.6
S164	BC-21	2.56	0.50	0.75	0.37	1.25	0.39	1.70	0.91	0.85	105.3
S165	BC-21	2.17	0.50	0.79	0.23	1.25	0.44	1.58	1.29	0.83	100.7
S166	BC-21	0.94	0.50	0.62	0.23	1.25	0.26	1.05	0.60	0.58	84.0
S167	BC-21	1.39	0.50	0.79	0.49	1.25	0.34	1.58	0.81	0.79	93.3
S168	BC-21	1.22	0.50	0.64	0.29	1.25	0.29	1.34	0.65	0.66	88.7
S169	BC-21	1.61	0.50	0.77	0.39	1.25	0.33	1.84	0.98	0.80	96.4
S170	BC-21	1.50	0.50	0.84	0.38	1.25	0.34	1.68	1.47	0.84	95.1
S171	BC-21	1.28	1.75	0.67	0.29	1.25	0.31	1.27	0.81	0.80	126.8
S172	BC-21	3.28	1.75	0.71	0.33	1.25	0.43	1.50	1.28	1.04	149.2
S173	BC-21	2.50	0.50	0.68	0.22	1.25	0.37	1.22	1.41	0.79	101.8
S174	BC-22	2.00	0.50	0.73	0.35	1.25	0.49	1.66	1.19	0.86	100.1
S175	BC-22	3.00	0.50	0.73	0.20	1.25	0.39	2.50	1.19	0.87	113.1
S176	BC-22	1.83	1.63	0.74	0.34	1.25	0.44	1.72	1.30	0.99	132.3
S177	BC-22	2.86	3.00	0.84	0.35	1.25	0.53	2.22	1.53	1.24	187.3
S178	BC-22	3.42	0.50	0.86	0.31	1.25	0.52	2.27	1.62	1.01	118.0
S179	BC-22	2.97	1.25	0.84	0.30	1.25	0.51	2.06	1.39	1.07	134.6
S180	BC-22	1.72	2.50	0.81	0.41	1.25	0.49	2.05	1.27	1.11	159.9
S181	BC-22	1.97	0.50	0.80	0.36	1.25	0.42	2.22	0.94	0.86	102.2
S182	BC-22	1.78	0.50	0.88	0.44	1.25	0.45	2.23	0.82	0.88	101.0
S183	BC-22	1.19	0.50	0.74	0.38	1.25	0.43	1.72	0.84	0.78	91.9
S184	BC-22	3.03	2.88	0.80	0.46	1.25	0.64	2.24	2.24	1.38	187.1
S185	BC-22	1.39	1.25	0.76	0.40	1.25	0.39	1.94	0.64	0.87	117.2
S186	BC-22	1.11	0.50	0.79	0.36	1.25	0.45	1.90	0.70	0.77	91.9
S187	BC-22	4.33	0.50	0.99	0.59	1.25	0.54	1.88	0.83	1.04	126.2
S188	BC-22	1.56	0.50	0.68	0.33	1.25	0.36	1.42	0.96	0.76	93.4
S189	BC-22	1.70	1.00	0.84	0.33	1.25	0.44	1.72	1.04	0.91	112.2
S190	BC-23	4.11	4.50	0.78	0.23	1.25	0.45	2.11	1.30	1.23	242.9
S191	BC-23	2.28	0.50	0.85	0.29	1.25	0.35	1.71	1.34	0.85	102.5
S192	BC-23	3.11	0.50	0.99	0.43	1.25	0.57	2.67	1.78	1.11	118.2
S193	BC-23	2.67	6.00	0.90	0.37	1.25	0.42	2.24	1.59	1.34	275.2
S194	BC-23	4.44	0.50	0.89	0.46	1.25	0.58	2.47	2.01	1.16	130.8
S195	BC-23	2.39	8.00	0.97	0.32	1.25	0.48	2.11	1.53	1.36	331.9
S196	BC-23	1.11	1.38	0.84	0.43	1.25	0.41	1.94	1.03	0.93	119.0
S197	BC-23	1.33	0.50	0.73	0.37	1.25	0.44	1.62	1.11	0.81	93.0
S198	BC-23	1.00	0.50	0.78	0.37	1.25	0.36	1.59	0.72	0.72	88.9
S199	BC-23	3.78	0.50	0.85	0.36	1.25	0.44	1.64	0.88	0.91	117.5
S200	BC-24	1.56	0.50	0.86	0.34	1.25	0.42	1.80	1.30	0.85	96.4
S201	BC-24	1.72	0.50	0.86	0.38	1.25	0.48	1.90	1.56	0.92	99.3
S202	BC-24	1.83	2.00	0.80	0.28	1.25	0.44	1.33	1.46	0.98	141.6
S203	BC-24	1.56	0.50	0.72	0.41	1.25	0.36	1.60	1.06	0.80	94.9
S204	BC-24	2.17	0.50	0.84	0.41	1.25	0.48	1.76	1.41	0.93	103.0
S205	BC-24	2.00	0.50	0.79	0.41	1.25	0.43	1.95	1.53	0.92	102.0
S206	BC-24	1.33	0.50	0.85	0.32	1.25	0.41	1.66	1.08	0.80	93.1
S207	BC-24	2.67	0.50	0.74	0.45	1.25	0.38	1.85	0.78	0.86	107.3
S208	BC-24	1.89	2.00	0.75	0.29	1.25	0.34	1.52	0.97	0.92	142.1

Table A3. *Cont.*

Sample	Borehole	CF_{As}	CF_{Cd}	CF_{Cr}	CF_{Cu}	CF_{Hg}	CF_{Ni}	CF_{Pb}	CF_{Zn}	PLI	RI
S209	BC-25	1.39	4.00	0.64	0.14	1.25	0.31	1.00	0.54	0.75	192.9
S210	BC-25	2.33	3.50	0.90	0.28	1.25	0.46	2.03	1.33	1.15	195.3
S211	BC-25	1.89	5.00	0.89	0.24	1.25	0.41	2.10	1.21	1.12	235.6
S212	BC-25	2.00	0.50	0.86	0.32	1.25	0.36	2.35	1.31	0.89	103.2
S213	BC-25	1.50	2.00	0.97	0.35	1.25	0.43	2.02	1.18	1.03	142.1
S214	BC-25	2.11	0.50	0.96	0.54	1.25	0.47	2.82	1.18	1.01	108.4
S215	BC-25	2.78	6.00	0.82	0.36	1.25	0.43	2.06	1.28	1.28	274.9
S216	BC-25	0.94	0.50	0.95	0.37	1.25	0.41	2.01	1.40	0.83	91.7
S217	BC-25	1.78	8.00	0.82	0.41	1.25	0.40	2.15	1.04	1.24	325.3
S218	BC-25	10.3	4.50	0.87	0.41	1.25	0.69	2.45	2.29	1.73	309.6
S219	BC-25	3.00	4.50	0.91	0.43	1.25	0.48	2.28	1.46	1.34	234.3
S220	BC-25	2.50	0.50	1.21	0.39	1.25	0.48	2.04	1.08	0.97	108.1
S221	BC-25	1.56	0.50	0.81	0.34	1.25	0.29	1.57	0.98	0.77	94.1
S222	BC-25	4.78	4.50	1.02	0.40	1.25	0.75	3.13	1.51	1.58	257.7
S223	BC-26	1.28	0.50	0.73	0.16	1.25	0.46	1.06	0.67	0.64	88.3
S224	BC-26	1.44	6.00	0.84	0.23	1.25	0.52	1.74	1.20	1.11	259.8
S225	BC-26	3.00	0.50	1.00	0.37	1.25	0.62	2.14	1.59	1.05	114.3
S226	BC-26	3.78	2.00	1.01	0.41	1.25	0.72	2.27	1.87	1.36	168.7
S227	BC-26	2.33	0.50	0.87	0.21	1.25	0.60	1.81	1.88	0.93	105.0
S228	BC-26	1.31	0.50	0.75	0.36	1.25	0.44	1.80	0.88	0.79	93.4
S229	BC-26	0.83	5.00	0.86	0.32	1.25	0.52	1.39	0.79	0.98	222.0
S230	BC-26	1.33	4.50	0.75	0.32	1.25	0.50	1.41	1.02	1.03	212.0
S231	BC-26	2.06	0.50	0.83	0.24	1.25	0.56	1.48	0.91	0.81	99.5
S232	BC-26	1.22	0.50	0.72	0.29	1.25	0.48	1.43	0.95	0.75	90.6
S233	BC-27	2.39	0.50	0.78	0.23	1.25	0.38	1.72	0.86	0.79	103.0
S234	BC-27	2.28	5.50	0.86	0.29	1.25	0.40	1.88	1.20	1.17	253.6
S235	BC-27	2.39	0.50	0.83	0.34	1.25	0.42	2.14	1.37	0.92	106.4
S236	BC-27	2.00	0.50	0.80	0.31	1.25	0.36	1.71	1.09	0.82	99.6
S237	BC-27	1.61	0.50	0.77	0.28	1.25	0.26	1.30	0.57	0.67	92.4
S238	BC-27	2.28	0.50	0.72	0.46	1.25	0.38	1.56	0.82	0.83	102.0
S239	BC-27	2.89	0.50	0.74	0.31	1.25	0.30	1.30	0.70	0.76	105.6
S240	BC-27	1.83	0.50	0.72	0.30	1.25	0.35	1.59	0.73	0.75	96.7
S241	BC-27	2.39	0.50	0.82	0.39	1.25	0.34	1.64	0.62	0.80	103.0
S242	BC-27	1.50	0.50	1.05	0.44	1.25	0.31	2.06	0.38	0.75	96.5
S243	BC-27	1.22	0.50	0.79	0.37	1.25	0.28	0.66	0.35	0.59	85.7
S244	BC-27	1.11	0.50	0.59	0.30	1.25	0.17	0.66	0.35	0.52	83.3
S245	BC-27	0.50	0.50	0.61	0.20	1.25	0.19	1.53	0.30	0.49	81.1
S246	BC-27	0.89	0.50	0.55	0.25	1.25	0.19	1.70	0.32	0.55	86.0
S247	BC-27	6.94	2.00	0.92	0.59	1.25	0.51	2.19	1.17	1.37	198.9
S248	BC-27	11.4	0.50	0.98	0.48	1.25	0.69	2.11	1.58	1.29	199.4
S249	BC-27	12.2	0.50	1.11	0.67	1.25	0.78	1.64	1.76	1.38	206.7
S250	BC-27	9.06	5.50	0.97	0.60	1.25	0.64	1.46	1.26	1.60	322.3

References

1. Veselinović, G.; Životić, D.; Penezić, K.; Kašanin-Grubin, M.; Mijatović, N.; Malbasić, J.; Sajnović, A. Geochemical characterization of sediments from the archaeological site Vinča-Belo Brdo, Serbia. *Catena* **2021**, *196*, 104914. [CrossRef]
2. Zhang, S.; Nwaila, G.T.; Bourdeau, J.E.; Ashwal, L.D. Machine learning-based prediction of trace element concentrations using data from the Karoo large igneous province and its application in prospectivity mapping. *Artif. Intell. Geosci.* **2021**, *2*, 60–75. [CrossRef]
3. Pavlović, P.; Kostić, N.; Karadžić, B.; Mitrović, M. The soils of Serbia. In *World Soils Book Series*; Hartemink, A.E., Ed.; Springer: Berlin/Heidelberg, Germany; Science + Business Media: Dordrecht, The Netherlands, 2017; ISBN 978-94-017-8659-1.
4. Rashid, A.; Schutte, B.J.; Ulery, A.; Deyholos, M.K.; Sanogo, S.; Lehnhoff, E.A.; Beck, L. Heavy Metal Contamination in Agricultural Soil: Environmental Pollutants Affecting Crop Health. *Agronomy* **2023**, *13*, 1521. [CrossRef]
5. Guo, Z.; Zhang, Y.; Xu, R.; Xie, H.; Xiao, X.; Peng, C. Contamination vertical distribution and key factors identification of metal (loid)s in site soil from an abandoned Pb/Zn smelter using machine learning. *Sci. Total Environ.* **2023**, *856*, 159264. [CrossRef]

6. Haghighizadeh, A.; Rajabi, O.; Nezarat, A.; Hajyani, Z.; Haghmohammadi, M.; Hedayatikhah, S.; Delnabi Asl, S.; Aghababai Beni, A. Comprehensive analysis of heavy metal soil contamination in mining environments: Impacts, monitoring techniques, and remediation strategies. *Arab. J. Chem.* **2024**, *17*, 105777. [CrossRef]
7. Zhu, Y.; Zhu, J.; Wang, B.; Xiao, M.; Li, L. Pollution characteristics and probabilistic health risk of potentially haz-ardous elements in soils near a typical coal mine in Panzhihua City, Southwest China. *Environ. Monit. Assess.* **2022**, *195*, 230. [CrossRef]
8. Wawrzonek, K.; Wątor, K.; Topolewski, M.; Kasprzak, A.; Kmiecik, E. Groundwater Potential in Mining Regions for Drinking Water Supply: A Case Study of the Żelatowa Intake (Chrzanów, Poland). *Water Resour. Ind.* **2024**, *32*, 100272. [CrossRef]
9. Chandra, G.V.; Ghosh, P.K. Groundwater quality in high-sulfur coal mining region of India: Spatial distribution, source control, and health risk assessment. *J. Environ. Manag.* **2024**, *368*, 122281. [CrossRef]
10. Giri, S.; Tiwari, A.K.; Mahato, M.K.; Singh, A.K. Spatio-temporal variations of metals in groundwater from an iron mining impacted area: Assessing sources and human health risk. *Total Environ. Res. Themes* **2023**, *8*, 100070. [CrossRef]
11. Angon, P.B.; Islam, M.S.; Shreejana, K.C.; Das, A.; Anjum, N.; Poudel, A.; Suchi, S.A. Sources, effects and present perspectives of heavy metals contamination: Soil, plants and human food chain. *Heliyon* **2024**, *10*, e28357. [CrossRef] [PubMed]
12. Song, Y.; Yang, Z. Vertical distributions and potential contamination assessment of seldom monitored trace elements in three different land use types of Yellow River Delta. *Mar. Pollut. Bull.* **2024**, *199*, 116033. [CrossRef] [PubMed]
13. Teh, T.L.; Rahman, N.N.N.A.; Shahadat, M.; Wong, Y.S.; Syakir, M.I.; Omar, A.M. A comparative study of metal contamination in soil using the borehole method. *Environ. Monit. Assess.* **2016**, *188*, 404. [CrossRef] [PubMed]
14. Sterckeman, T.; Douay, F.; Proix, N.; Fourrier, H. Vertical distribution of Cd, Pb and Zn in soils near smelters in the North of France. *Environ. Pollut.* **2000**, *107*, 377–389. [CrossRef]
15. Đorđević, D.; Tadić, J.M.; Grgur, B.; Ristić, R.; Sakan, S.; Brezjanović, J.; Stevanović, V.; Šolaja, B. The influence of exploration activities of a potential lithium mine to the environment in Western Serbia. *Sci. Rep.* **2024**, *14*, 17090. [CrossRef]
16. Geological Survey of Serbia. 2021. Potencijalnost Republike Srbije sa Aspekta Podzemnih Voda i Geotermalnih Resursa, Republic of Serbia. Available online: https://www.google.com/url?sa=t&source=web&rct=j&opi=89978449&url=https://www.gzs.gov.rs/doc/Potenc-RS-sa-aspek-podzemnih-voda-i-geotermalnih-resursa-2021-(00000003).pdf&ved=2ahUKEwj507D7hfWIAxXV3wIHHV24FZMQFnoECBcQAQ&usg=AOvVaw1SW3QOIoz0Xejt-5MXpFT0 (accessed on 18 November 2024). (In Serbian)
17. Živanović, V.; Joksimović, M.; Golić, R.; Malinić, V.; Krstić, F.; Sedlak, M.; Kovjanić, A. Depopulated and Abandoned Areas in Serbia in the 21st Century—From a Local to a National Problem. *Sustainability* **2022**, *14*, 10765. [CrossRef]
18. Čakmak, D.; Perović, V.; Antić-Mladenović, S.; Kresović, M.; Saljnikov, E.; Mitrović, M.; Pavlović, P. Contamination, risk, and source apportionment of potentially toxic microelements in river sediments and soil after extreme flooding in the Kolubara River catchment in Western Serbia. *J. Soils Sediments* **2018**, *18*, 1981–1993. [CrossRef]
19. Šajn, R.; Aliu, M.; Stafilov, T.; Alijagić, J. Heavy metal contamination of topsoil around a lead and zinc smelter in Kosovska Mitrovica/Mitrovicë, Kosovo/Kosovë. *J. Geochem. Explor.* **2013**, *134*, 1–16. [CrossRef]
20. Antunović, V.; Blagojević, D.; Baošić, R.; Relić, D.; Lolić, A. Health risk assessment of heavy metals in soil, plant, and water samples near "Gacko" power plant, in Bosnia and Herzegovina. *Environ. Monit. Assess.* **2023**, *195*, 596. [CrossRef]
21. Radomirović, M.; Ćirović, Ž.; Maksin, D.; Bakić, T.; Lukić, J.; Stanković, S.; Onjia, A. Ecological risk assessment of heavy metals in the soil at a former painting industry facility. *Front. Environ. Sci.* **2020**, *8*, 560415. [CrossRef]
22. Martinović, M.; Ratkaj, I. Sustainable rural development in Serbia: Towards a quantitative typology of rural areas. *Carpath. J. Earth Environ. Sci.* **2015**, *10*, 37–48.
23. Ranđelović, D.; Mutić, J.; Marjanović, P.; Đorđević, T.; Kašanin-Grubin, M. Geochemical distribution of selected elements in flotation tailings and soils/sediments from the dam spill at the abandoned antimony mine Stolice, Serbia. *Environ. Sci. Pollut. Res.* **2019**, *27*, 6253–6268. [CrossRef] [PubMed]
24. Đukičin, S.; Đorđević, S.; Milanković, J. Spatial and social changes caused by the continuous exploitation of lignite in the Kolubara lignite basin, Serbia. *Acta Geogr. Slov.* **2014**, *54*, 77–88. [CrossRef]
25. Wang, X.; Li, L.; Yan, X.; Meng, X.; Chen, Y. Processes of chromium (VI) migration and transformation in chromate production site: A case study from the middle of China. *Chemosphere* **2020**, *257*, 127282. [CrossRef]
26. Milanović, S.; Stevanović, Z.; Đurić, D.; Petrović, T.; Milovanović, M.; Mandić, M. Karta Ugroženosti Podzemnih Voda Srbije/Map of Groundwater Threats in Serbia. 2011. Available online: https://geoliss.mre.gov.rs/prez/KartaUgrPodVodWeb/index.html (accessed on 4 October 2024). (In Serbian)
27. Vasić, M.V.; Pezo, L.; Vasić, M.R.; Mijatović, N.; Mitrić, M.; Radojević, Z. What is the most relevant method for water absorption determination in ceramic tiles produced by illitic-kaolinitic clays? The mystery behind the gresification diagram. *Bol. Soc. Esp. Ceram. Vidr.* **2022**, *61*, 241–251. [CrossRef]
28. The State of Soil Report in the Republic of Serbia. 2016–2017. Available online: https://sepa.gov.rs/wp-content/uploads/2024/10/Zemljiste-2016-2017.pdf (accessed on 11 December 2024).
29. Mijatović, N.; Vasić, M.; Miličić, L.; Radomirović, M.; Radojević, Z. Fired pressed pellet as a sample preparation technique of choice for an energy dispersive X-ray fluorescence analysis of raw clays. *Talanta* **2023**, *252*, 123844. [CrossRef] [PubMed]
30. Radomirović, M.; Mijatović, N.; Vasić, M.; Tanaskovski, B.; Mandić, M.; Pezo, L.; Onjia, A. The characterization and pollution status of the surface sediment in the Boka Kotorska Bay, Montenegro. *Environ. Sci. Pollut. Res.* **2021**, *28*, 53629–53652. [CrossRef] [PubMed]

31. Karim, K.N.; Tsikouras, B.; Ifandi, E.; Lai, C.-K.; Osli, L.N.; Shalaby, M.R.; Islam, M.A. Geochemical baselines of potentially toxic elements in Brunei-Muara soils, Brunei Darussalam: Towards environmental assessment and risk management. *J. Geochem. Explor.* **2024**, *257*, 107382. [CrossRef]
32. Wang, C.; Li, W.; Yang, Z.; Chen, Y.; Shao, W.; Ji, J. An invisible soil acidification: Critical role of soil carbonate and its impact on heavy metal bioavailability. *Sci. Rep.* **2015**, *31*, 12735. [CrossRef] [PubMed]
33. Wang, X.-S.; Qin, Y.; Chen, Y.-K. Heavy metals in urban roadside soils. Part 1: Effect of particle size fractions on heavy metals partitioning. *Environ. Geol.* **2006**, *50*, 1061–1066. [CrossRef]
34. Chen, X.; Lewis, S.; Heal, K.V.; Lin, Q.; Sohi, S.P. Biochar engineering and ageing influence the spatiotemporal dynamics of soil pH in the charosphere. *Geoderma* **2021**, *386*, 114919. [CrossRef]
35. Chen, Y.; Hu, C.; Deng, D.; Li, Y.; Luo, L. Factors affecting sorption behaviors of tetracycline to soils: Importance of soil organic carbon, pH and Cd contamination. *Ecotoxicol. Environ. Saf.* **2020**, *197*, 110572. [CrossRef]
36. Kicińska, A.; Pomykała, R.; Izquierdo-Diaz, M. Changes in soil pH and mobility of heavy metals in contaminated soils. *Eur. J. Soil Sci.* **2022**, *73*, e13203. [CrossRef]
37. Răcușan Ghircoiaș, O.; Tănăselia, C.; Chintoanu, M.; Crișan, I.; Hoble, A.; Ștefan, R.; Dîrja, M. Relevance of Soil Heavy Metal XRF Screening for Quality and Landscaping of Public Playgrounds. *Toxics* **2023**, *11*, 530. [CrossRef]
38. Håkanson, L. An ecological risk index for aquatic pollution control. A sedimentological approach. *Water Res.* **1980**, *14*, 975–1001. [CrossRef]
39. Taylor, S.R. Abundance of chemical elements in the continental crust: A new table. *Geochim. Cosmochim. Acta* **1964**, *28*, 1273–1285. [CrossRef]
40. Miletić, A.; Radomirović, M.; Đorđević, Đ.; Bogosavljević, J.; Lučić, M.; Onjia, A. Geospatial mapping of ecological risk from potentially toxic elements in soil in the Pannonian-Carpathian border area south of the Danube. *Carpathian J. Earth Environ. Sci.* **2022**, *17*, 351–363. [CrossRef]
41. Sahoo, P.K.; Equeenuddin, S.M.; Powell, M.A. Trace Elements in Soils around Coal Mines: Current Scenario, Impact and Available Techniques for Management. *Curr. Pollut. Rep.* **2016**, *2*, 1–14. [CrossRef]
42. Aytop, H.; Ateş, Ö.; Dengiz, O.; Yılmaz, C.H.; Demir, Ö.F. Environmental, ecological and health risks of boron in agricultural soils of Amik Plain under Mediterranean conditions. *Stoch. Environ. Res. Risk Assess.* **2023**, *37*, 2069–2081. [CrossRef]
43. Jiang, H.H.; Cai, L.M.; Wen, H.H.; Hu, G.C.; Chen, L.G.; Luo, J. An integrated approach to quan tifying ecological and human health risks from different sources of soil heavy metals. *Sci. Total Environ.* **2019**, *701*, 134466. [CrossRef] [PubMed]
44. Hoang, H.G.; Lin, C.; Chiang, C.F.; Bui, X.T.; Lukkhasorn, W.; Bui, T.P.T.; Tran, H.T.; Vo, T.D.H.; Le, V.G.; Nghiem, L.D. The individual and synergistic indexes for assessments of heavy metal contamination in global rivers and risk: A review. *Curr. Poll. Rep.* **2021**, *7*, 247–262. [CrossRef]
45. Tomlinson, D.L.; Wilson, J.G.; Harris, C.R.; Jefrey, D.W. Problems in the assessment of heavy-metal levels in estuaries and the formation of a pollution index. *Helgoländer Meeresunters.* **1980**, *33*, 566–575. [CrossRef]
46. Carrillo, K.C.; Rodríguez-Romero, A.; Tovar-Sánchez, A.; Ruiz-Gutiérre, G.; Viguri Fuente, J.R. Geochemical baseline establishment, contamination level and ecological risk assessment of metals and As in the Limoncocha lagoon sediments, Ecuadorian Amazon region. *J. Soils Sediments* **2022**, *22*, 293–315. [CrossRef]
47. Starbuck, C. Descriptive Statistics. In *The Fundamentals of People Analytics*; Springer: Cham, Switzerland, 2023. [CrossRef]
48. Arsenović, M.; Pezo, L.; Vasić, N.; Ćirić, R.; Stefanović, M. The main factors influencing canine demodicosis treatment outcome and determination of optimal therapy. *Parasitol. Res.* **2015**, *114*, 2415–2426. [CrossRef]
49. Hammam, A.A.; Mohamed, W.S.; Sayed, S.E.-E.; Kucher, D.E.; Mohamed, E.S. Assessment of Soil Contamination Using GIS and Multi-Variate Analysis: A Case Study in El-Minia Governorate, Egypt. *Agronomy* **2022**, *12*, 1197. [CrossRef]
50. Stanković, S.; Tanaskovski, B.; Zlatić, B.; Arsenović, M.; Pezo, L. Analysis of trace elements in surface sediments, mussels, seagrass and seawater along the southeastern Adriatic coast—A chemometric approach. *Pure Appl. Chem.* **2014**, *86*, 1111–1127. [CrossRef]
51. Štrbac, S.; Stojić, N.; Lončar, B.; Pezo, L.; Ćurčić, L.; Prokić, D.; Pucarević, M. Heavy metal concentrations in the soil near illegal landfills in the vicinity of agricultural areas—Artificial neural network approach. *J. Soils Sediments* **2024**, *24*, 373–389. [CrossRef]
52. Official Gazette of the Republic of Serbia. (Službeni glasnik Republike Srbije) The Rule Book on Permitted Quantities of Dangerous and Harmful Substances in Land and Water for Irrigation and Methods of Their Testing (Pravilnik o dozvoljenim količinama opasnih i štetnih materija u zemljištu i vodi za navodnjavanje i metodama njihovog ispitivanja), No. 88/2010. 1994. Available online: http://demo.paragraf.rs/demo/combined/Old/t/t2008_12/t12_0236.htm (accessed on 15 December 2024).
53. Official Gazette of the Republic of Serbia. (Službeni glasnik Republike Srbije) Regulation on the Program of Systematic Monitoring of Land Quality, Indicators for Assessing the Risk of Land Degradation and Methodology for the Development of Remediation Programs (Uredba o programu sistemskog praćenja kvaliteta zemljišta, indikatorima za ocenu rizika od degradacije zemljišta i metodologiji za izradu remedijacionih programa), No. 88/2010, In Serbian. 2010. Available online: https://www.paragraf.rs/propisi/uredba-sistematskom-pracenju-stanja-kvaliteta-zemljista.html (accessed on 15 December 2024).
54. Official Gazette of the Republic of Serbia. (Službeni glasnik Republike Srbije) Regulation on Limit Values of Pollutants, Harmful and Hazardous Substances in Soil (Uredba o graničnim vrednostima zagađujućih, štetnih i opasnih materija u zemljištu), Official Gazette of Republic of Serbia, No. 30/2018 and No. 64/2019, in Serbian. 2018–2019. Available online: https://www.paragraf.rs/propisi/uredba-granicnim-vrednostima-zagadjujucih-stetnih-opasnih-materija-zemljistu.html (accessed on 15 December 2024).

55. Dutch Target and Intervention Values. Circular on Target Values and Intervention Values for Remediation. Dutch Ministry of Housing, Spatial Planning and Environment, Netherlands Government Gazette: 2000. Available online: https://support.esdat.net/Environmental%20Standards/dutch/annexs_i2000dutch%20environmental%20standards.pdf (accessed on 15 December 2024).
56. Dugalic, G.; Krstic, D.; Jelic, M.; Nikezic, D.; Milenkovic, B.; Pucarevic, M.; Zeremski-Skoric, T. Heavy metals, organics and radioactivity in soil of western Serbia. *J. Haz. Mat.* **2010**, *177*, 697–702. [CrossRef] [PubMed]
57. Xie, Z.M.; Lu, S.G. Trace elements and environmental quality. In *Micronutrients and Biohealth*; Wu, Q.L., Ed.; Guizhou Science Technology Press: Guiyang, China, 2007; pp. 208–216.
58. Manojlović, M.; Ram Singh, B. Trace elements in soils and food chains of the Balkan region. *Acta Agric. Scand. B* **2012**, *62*, 8. [CrossRef]
59. Report on The State of Soil in the Republic of Serbia (Izveštaj o stanju zemjišta u Republici Srbiji). 2018–2019. In Serbian. Available online: https://degradacijazemljista.sepa.gov.rs/?p=1293 (accessed on 15 December 2024).
60. Jia, Y.; Yang, X.; Yan, X.; Duguer, W.; Hu, H.; Chen, J. Accumulation, potential risk and source identification of toxic metal elements in soil: A case study of a coal-fired power plant in Western China. *Environ. Geochem. Health* **2023**, *45*, 7389–7404. [CrossRef] [PubMed]
61. Vaněk, A.; Chrastný, V.; Komárek, M.; Galušková, I.; Drahota, P.; Grygar, T.; Tejnecký, V.; Drábek, O. Thallium dynamics in contrasting light sandy soils—Soil vulnerability assessment to anthropogenic contamination. *J. Hazard. Mater.* **2010**, *173*, 717–723. [CrossRef] [PubMed]
62. Jacobson, A.R.; McBride, M.B.; Baveye, P.; Steenhuis, T.S. Environmental factors determining the trace-level sorption of silver and thallium to soils. *Sci. Total Environ.* **2005**, *345*, 191–205. [CrossRef] [PubMed]
63. Xiao, T.; Guha, J.; Boyle, D.; Liu, C.-Q.; Chen, J. Environmental concerns related to high thallium levels in soils and thallium uptake by plants in southwest Guizhou, China. *Sci. Total Environ.* **2004**, *318*, 223–244. [CrossRef]
64. Wnuk, E. Mobility, bioavailability, and toxicity of vanadium regulated by physicochemical and biological properties of the soil. *J. Soil Sci. Plant Nutr.* **2023**, *23*, 1386–1396. [CrossRef]
65. Cappuyns, V. Barium (Ba) leaching from soils and certified reference materials. *Appl. Geochem.* **2018**, *88*, 68–84. [CrossRef]
66. Zhang, Y.; Li, L.; Song, B.; Xu, R.; Zhou, Z.; Zhu, L.; Zhou, L. Comprehensive Risk Assessment of Heavy Metals Based on Pollution Sources: A Case Study for Agricultural Soils from Southwest China. *Expo. Health* **2024**, 1–16. [CrossRef]
67. Vasić, M.V.; Velasco, P.M.; Mijatović, N.; Radormirović, M.; Radojević, Z. Sustainable approach to raw clays for ceramic and refractory applications: Insights from updated traditional ternary diagrams. *Clay Min.* **2024**, *59*, 202–212. [CrossRef]
68. Stevanović, Z.; Marinović, V.; Merdan, S.; Skopljak, F.; Jolović, B. Conception of Creating Basic Documents in Hydrogeology for River Basin Management Plans. I Kongres Geologa Bosne i Hercegovine, Tuzla. 2015. Available online: https://acrobat.adobe.com/id/urn:aaid:sc:EU:0a53e4a6-a880-4205-95c3-fbb48d2c7558?viewer!megaVerb=group-discover (accessed on 10 February 2024).

Disclaimer/Publisher's Note: The statements, opinions and data contained in all publications are solely those of the individual author(s) and contributor(s) and not of MDPI and/or the editor(s). MDPI and/or the editor(s) disclaim responsibility for any injury to people or property resulting from any ideas, methods, instructions or products referred to in the content.